

## ABSTRACT

Aquifer Framework Restoration (AFR) in an Alluvial Aquifer, Central Texas

David H. Ju, M.S.

Mentor: Joe Yelderian Jr., Ph.D.

The Brazos River Alluvium aquifer (BRAA) near Waco, Texas is an aquifer whose framework has been physically impacted by sand and gravel mining. The most productive portions of the BRAA framework are being excavated and kept as pit lakes or filled with different material. GIS identification of mined areas was estimated to cover 4.4% of the BRAA from which evaporative losses was calculated to be 10% of average annual recharge. Permeameter tests suggest that foreign material comprised of large limestone gravel or construction debris has high K and implications to improve production compared to fine grained native (overburden) fill. Construction debris had elevated sulfate and magnesium signatures that were found to decrease from weathering over time. Groundwater models showed foreign and native materials to on average increase and decrease groundwater flow respectively. Characterization of fill material is essential for Aquifer Framework Restoration (AFR).

Aquifer Framework Restoration (AFR) in an Alluvial Aquifer, Central Texas

by

David H. Ju, B.S.

A Thesis

Approved by the Department of Geology

---

Stacy Atchley, Ph.D., Chairperson

Submitted to the Graduate Faculty of  
Baylor University in Partial Fulfillment of the  
Requirements for the Degree  
of  
Master of Science

Approved by the Thesis Committee

---

Joe C. Yelderman Jr., Ph.D., Chairperson

---

Peter M. Allen, Ph.D.

---

Sascha Usenko, Ph.D.

Accepted by the Graduate School

August 2014

---

J. Larry Lyon, Ph.D., Dean

Copyright © 2014 by David H. Ju

All rights reserved

## TABLE OF CONTENTS

CHAPTER ONE	1
Background	1
<i>Sand and Gravel Demands</i>	1
<i>Gravel Pits and Fill Material</i>	2
<i>Problem with open pits</i>	2
<i>Groundwater regulation</i>	4
<i>Remediation Reclamation and Restoration</i>	5
<i>Aquifer restoration</i>	5
<i>Wetland restoration</i>	6
<i>Stream restoration</i>	6
<i>Purpose</i>	7
<i>Location</i>	8
<i>Geologic Setting</i>	9
<i>Hydrogeologic Setting</i>	12
CHAPTER TWO	14
Methods	14
<i>Geospatial</i>	14
<i>Laboratory</i>	15
<i>Permeameter</i>	15
<i>Chemical Analysis</i>	17
<i>Field</i>	18
<i>Resistivity</i>	18
<i>Bore Hole</i>	19
<i>Finite Difference Modeling</i>	20
CHAPTER THREE	22
Results and Discussion	22
<i>Geospatial</i>	22
<i>Laboratory</i>	27
<i>Sample Collection and Description</i>	27
<i>Permeameter</i>	33
<i>Chemical Analysis</i>	37
<i>Field</i>	43
<i>Resistivity</i>	43
<i>Finite Difference Modeling</i>	49
<i>Model Setup</i>	49
<i>Model Scenarios</i>	51

CHAPTER FOUR	63
Summary and Conclusions	63
CHAPTER FIVE	65
Recommendations	65
APPENDICES	66
Appendix A Porosity Measurements for Fine-grained Samples	67
Appendix B Well Data	69
Appendix C Chemical Data	75
REFERENCES CITED	78

## LIST OF FIGURES

Figure		Page
Figure 1	Study location map.	9
Figure 2	Geologic map.	11
Figure 3	Photograph of a gravel pit wall	13
Figure 4	Flow chart illustrating the steps taken	15
Figure 5	Modified large bucket permeameter.	16
Figure 6	Resistivity survey in the field.	19
Figure 7	Drill rig with four-inch auger stem drill.	20
Figure 8	Spatial analysis of the BRAA.	23
Figure 9	Annual rainfall for Waco, Texas from 1976-2012.	24
Figure 10	Field sample collection locations.	28
Figure 11	Examples of collection sites.	29
Figure 12	General description of aquifer material and native material	31
Figure 13	Description of foreign materials	32
Figure 14	Hydraulic conductivity of unconsolidated material.	34
Figure 15	Piper diagram to determining water type.	38
Figure 16	Concentration fluctuations of fresh concrete and brick material over three exposures.	41
Figure 17	Comparison between fresh concrete and weathered concrete.	42
Figure 18	Aerial photographs of the resistivity survey area.	45
Figure 19	Resistivity profiles near a filled gravel pit. The A series.	46
Figure 20	Resistivity profiles near a filled gravel pit. The B series.	47

Figure 21	Finite difference groundwater grid created in MODEL MUSE.	52
Figure 22	Head contour map of scenario one (pre-mining)	54
Figure 23	Head contour map of scenario two (pit lakes)	55
Figure 24	Head contour map of scenario three (native fill)	58
Figure 25	Head contour map of scenario four (foreign fill)	60
Figure 26	Composite of travel time graphs for all four scenarios.	61
Figure B1	Well-1 used to field check resistivity surveys	70
Figure B2	Well-1 used to field check resistivity surveys	71
Figure C1	Comparison of analyzed water data	76

## LIST OF TABLES

Table		Page
Table 1	Hydrogeologic data of the BRAA found in the literature.	13
Table 2	Water budget for the BRAA with in McLennan County.	27
Table 3	Average hydraulic conductivity for samples	34
Table 4	Ionic concentrations given in mg/l, pH, and Ec ( $\mu$ S).	37
Table A1	Porosity calculations for fine-grained material	68
Table B1	Well completion data for two wells	73
Table B2	Model calibration wells	73
Table B3	Estimated particle travel time	75
Table C1	Min, mean, and max ion concentrations	77

## ACKNOWLEDGMENTS

I would like to give thanks to my parents for teaching me to endure the challenges of life with faith, courage, and strength. To be humble in times of prosperity but wise enough to enjoy the moment. I extend gratitude to friends and colleagues, for assisting me in fieldwork, sharing life experiences, and enriching my graduate experience. fieldwork was conducted near the water treatment plant (Robinson, TX.) and the Hirsh Dairy land. Field Permission to drill boreholes was made possible only by their generosity and ideals to further education.

I am blessed to have passionate and dedicated educators instill the desire for science in me. Through knowledge and gentle criticism, sharp focus and eclectic understanding, and with close watch and unabated idea my character, ability, and self-confidence grew. This thesis would not have been possible without the support of Dr. Joe C. Yelderman. His guidance and belief in me gave me the fortitude needed to endure. Finally, the utmost appreciativeness to God, whom through Him all of this was possible.

## CHAPTER ONE

### Background

Aquifers account for more than half of the water supply in Texas, with some of the most productive sources being alluvial aquifers (Bureau of Economic Geology 2004). The Brazos River Alluvium aquifer (BRAA) is a shallow water table aquifer able to supply water for irrigation, domestic, livestock, and commercial use (Shah 2007). This aquifer was down-graded from a major aquifer to one of 21 minor aquifers in the State because it is primarily used for agriculture and has relatively low production (Ashworth and Hopkins 1995). Urbanization on the floodplain covers recharge zones and uses mineral resources mined out of the framework of the alluvial aquifer for building material (Morgan-Jones and others 1984). The framework of the BRAA, the alluvium, is a source of sand, gravel and fill material used in general construction, here after referred to as “gravel”.

#### *Sand and Gravel Demands*

Texas is the second largest producer of Gravel removal in shallow alluvial aquifers physically removes the aquifer framework. The high demand for gravel has left pits filled naturally with water or manually filled with other materials (Morgan-Jones and others 1984). The physically altered aquifer, whether a pit is filled or unfilled, may no longer support its original functionality. However, some materials used to fill gravel pits may have properties that could mimic or increase the production potential of the original aquifer framework. These materials could be used to replace the lost aquifer framework.

### *Gravel Pits and Fill Materials*

Initially, the hydrogeological behavior in gravel pits is dictated by the floor elevation relative to the water table (Younger and others 2002). In one scenario, the elevation of the pit floor is higher than the water table and in the second scenario, the base of the pit is submerged below the water table. The former has been observed to perch water above the water table. The latter are considered “through flow” lakes allowing water to enter the pit lake by lateral groundwater inflow, precipitation and surface runoff and recharge back into the aquifer in the down gradient side (Morgan-Jones, Bennett, and Kinsella 1984). In this study, all identified mines are assumed to be excavated to the bedrock and are classified as through-flow lakes to simplify calculations.

### *Problem with Open Pits*

Evaporative effects on pit lakes are known to lose more water than the effects of evapotranspiration from vegetation on unexcavated land (Grandy and others 2004). Evaporation in pit lakes also increases the concentration of solutes (Younger and others 2002). Studies finding evapotranspiration to be a greater groundwater sink than lake evaporation has been interpreted to be the result of specific climate conditions (Grandy and others 2004). The evaporation causes drawdown, which lowers the head within the pit lake shifting local flow towards them (Hobbs and Gunn 1998).

### *Groundwater Regulations.*

Hatva (1994) studied the effect of gravel pits on groundwater in Finland. He found that anthropogenic factors impacting the groundwater included location, pumpage, and dumping of waste (Hatva 1994). Groundwater resources in his study location

(Finland) were protected with zoning that restricts gravel extraction below the water table in areas classified as important (Hatva 1994).

The clean water act of 1972 was amended to restore and maintain the chemical, physical, and biological integrity of the nation's waters (92nd United States Congress 1972). This amendment, along with many amendment to follow, often protects groundwater from being polluted but does not regulate the material groundwater moves through. Regulations that specifically relate to gravel mining practices vary by state. Under Texas Administrative Code, Natural Resources and Conservation (title 31), General Land Office (part) 1, and chapter 10 titled exploration and development of mineral resources other than oil and gas, rule 10.7, mining reclamation is loosely enforced. For example, the code states,

If subsurface excavation is planned, a statement of what possible effect such excavations could have on water, as defined by Texas Civil Statutes, Article 8866, §1(11) (Vernon, 1989). The code also requires, "a specification of what reclamation efforts will be undertaken to minimize the impact of operations on the surface, including vegetation, topsoil, wildlife habitats, caused by operations.

Water is, in this case, referring to navigable surface waters. Many statements in the code verbalize the desire to reclaim the surface soil, vegetation, water and wildlife. Mention of the subsurface in connection to groundwater restoration is sparse but absolutely clear.

The statements regarding groundwater state,

Determine whether full restoration, including spreading of topsoil stockpile, of all areas disturbed during permitted activity to preoperation elevations, contours, and substrata should be required (92nd United States Congress 1972).

Use of the word restoration instead of reclamation is deliberate and expresses a need for complete restoration. In order to re-grade the pit lake to preoperation elevations the code states,

All waste rock, deleterious materials or substances and other waste produced by operations shall be deployed, arranged, disposed of, or treated in accordance with federal and state requirements and so as to minimize adverse impact upon the environment and surface resources. (92nd United States Congress 1972).

Morgan-Jones and others (1984) and Graf (2004) are two articles found to deal specifically with gravel mining and their effects on aquifer hydrogeology. Morgan-Jones and others (1984) described the hydraulic effect of water filled pits and pits filled with waste material. He described water filled pits as areas of high K, which established lower up-gradient water levels and higher down-gradient levels. Poorly controlled infilling with highly pollutant to inert spoils has been found to impede the groundwater in floodplains near London (Morgan-Jones and others 1984). He also concluded that movement of land-fill leachate was worsened by pumping activity in adjacent pit lakes. The exact material used for infilling, labeled as “waste”, is not known but suggest that infilling materials are less permeable than the surrounding sand and gravel leading to higher up-gradient water levels and lower down-gradient levels. Urbanc (2005) took a chemical and geographical approach to investigate illegal dumping in gravel pits, which included identifying illegal dumps in gravel pits, describing the fill, and testing the groundwater beneath the fill. The fill material was mostly non-hazardous construction debris (Urbanc 2005).

In conjunction with gravel mining and infilling, Yelderman and Cervenka (1993) studied the environment of McLennan County and suggested reclamation of all surface excavations to maintain land value and decrease hazard. Reclamation during the mining operation is advised in order to avoid new vegetative growth that may be more difficult to remove later, and to plan for urban development.

### *Remediation, Reclamation, and Restoration*

Remediation, reclamation, and restoration generally refer to activities that attempt to improve the current use of a degraded site (Finger, Church, and von Guerard 2007). These activities are similar but have different goals and various degrees of difficulty to achieve. Remediation refers to the cleanup of contaminants and reclamation is a repurposing of the land for a beneficial use (Finger and others 2007). According to the National Research Council and its report on aquatic ecosystems, restoration is an attempt to return an ecosystem to near pristine conditions prior to physical or chemical disturbance (National Research Council 1992).

#### *Aquifer Restoration*

The majority of aquifer restoration studies have focused on water quality, similar to remediation (Canter 1982; Crystal and Heeley 1983; Castro and Moore 2000). Physical degradation of aquifer structure is recognized in the literature, but scarcely the focus of restoration studies (Urbanc and Berg 2005; Morgan-Jones and others 1984; Grandy and others 2004). Often the only literature regarding management of gravel-mined aquifers specifically is found in State and County reports, as it is generally a local concern (Grandy and others 2004). Reclaiming pit lakes by infilling or repurposing for wildlife and recreation is commonly practiced but does not address the physical degradation to the aquifer (Buttleman 1992; Morgan-Jones and others 1984). Aquifers have not been a common subject in restoration because efforts may be extremely difficult, expensive, and invisible (Rich 1983). More common wetland and stream restorations studies were researched to extract knowledge about successful restorations applicable to aquifers.

### *Wetland Restoration*

Wetland and stream restoration in the literature have illustrated a few critical components of environmental restoration applicable to aquifers. A study by Maguire (1985) found that only 50% of the 23 wetlands studied in Florida were successful using vegetation cover and implementation of permit conditions to estimate mitigation success. Wetland restoration has a stigma of using easily measured parameters such as plants species, animal abundance, and vegetation cover as indicators of success (Mitsch and Wilson 1996). Likewise Erwin (1991) found similar results in their study of 40 sites in Florida where 24 (60%) of the projects studied were judged to be incomplete or failures. Mitsch and Wilson (1996) suggest that a relatively high number of “failures” of mitigation wetlands can be attributed to the general lack of understanding of wetland science. Some researchers, like Mitsch (1995), suggest isolating functional requirements for achieving success of wetland creation and restoration projects: understanding wetland function, giving the system time, better monitoring, and letting the wetland grow as naturally as possible. Recreating the structure and functionality of wetlands seems easily reachable but the reality is wetland ecosystems, and many other systems alike, have complexities that are nearly impossible to predict (Zedler 1999). Zedler also suggests that prevention and early detection of degradation is a much more realistic application in restorative sciences.

### *Stream Restoration*

Abundant deposits of sand and gravel can be found associated with streams. Extraction of these raw materials from their streambeds can significantly alter the physical, chemical and biological characteristics of mined streams (Nelson 1993). Gravel

mining on floodplains has produced severe channel alterations resulting in elimination or reduction of the fish populations (Woodward-Clyde Consultants 1980). These examples illustrate a relationship between the physical framework and the ecosystem.

Restoration failures can be minimize by recognizing components of bad design from a literature search. Wetland and stream studies often stress the importance for the ecosystems to work physically before the biota can thrive. Urbanc (2005) suggested remediation techniques, one of which may be able to restore some physical framework for gravel pits. He states that anthropogenic remediation has the option to fill the pit and/or plant trees. The idea to simply leave the inert construction debris in the pit and level it was suggested (Urbanc 2005). Construction materials are commonly found dumped in gravel pits. The permeability of construction rubble has not been studied a great deal in the literature. Purposeful application of construction debris could be used to restore the aquifer framework, increase production and protect groundwater.

### *Purpose*

There is a lack of knowledge concerning foreign materials used to fill open pits occurring in aquifers. There is little known about the foreign materials effects on groundwater chemistry or aquifer functionality. The purpose of this study is to advance our understanding of materials used to fill mined pits that may improve aquifer framework restoration (AFR) efforts. Key objectives regarding aquifer restoration in this study include:

- 1. Establish the current state of annual recharge by estimate the recharge of the BRAA with anthropogenic influences.*

2. *Characterize the materials that are used to fill depressions in the BRAA by identifying the physical and chemical properties of materials occupying mined areas.*
3. *Observe the aquifer response caused by gravel mining operations by modeling the BRAA using MODFLOW 2005.*

### *Location*

McLennan County and the City of Waco are located in Central Texas. The Brazos River is a prominent feature, which runs through McLennan County from the northwest to southeast. The BRAA will here after refer to the aquifer within the study area, which is defined by the BRAA within McLennan County (figure 1).

Yelderman and Cervenka (1993) developed The Environmental Atlas of McLennan County for use in future planning. The atlas describes environmental conditions in McLennan County centered on the major urban community, the City of Waco. The Brazos River floodplain and associated lower terraces are characterized as topographically flat to gently rolling, with open land, deciduous and post oak growth. The majority of the soil on the floodplain is poorly developed because it is young. Urban development on the floodplain is cautioned with low bearing capacity, high shrink-swell properties, and flooding. Yelderman and Cervenka (1993) observed the tendency for urban development to be adjacent to operating or abandoned pits along the BRAA.

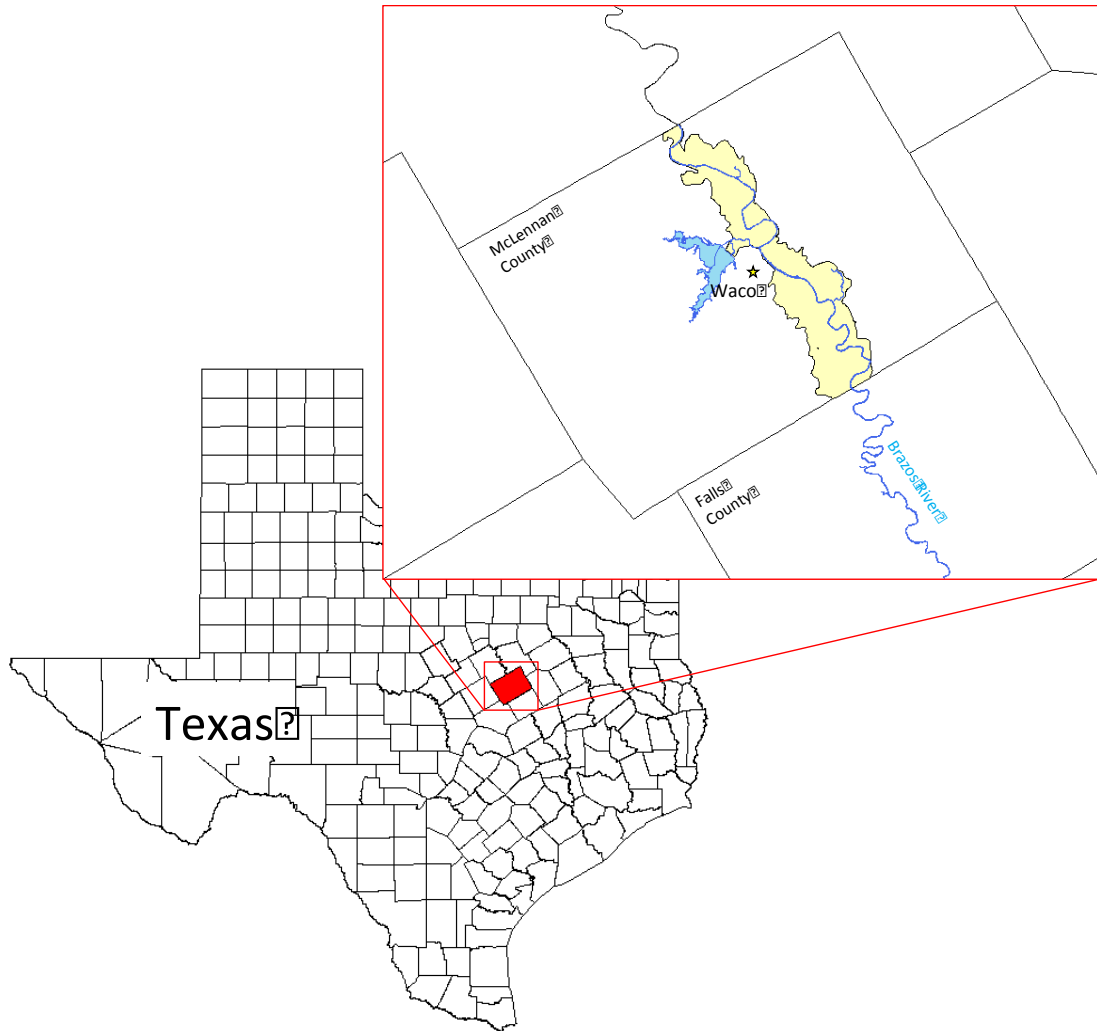


Figure 1 Location map showing McLennan County (red) within the state of Texas. The study focuses on the Brazos River Alluvium Aquifer (yellow) within McLennan County near Waco, TX.

### *Geologic Setting*

The BRAA is comprised of Brazos River floodplain alluvium and paleo-Brazos River terrace alluvium deposited on top of Cretaceous bedrock (J. Cronin and Wilson 1967). Glacial melts during the Pleistocene are associated with the deposition and erosion of multiple floodplain layers (Epps 1973). The Cretaceous bedrock is associated with shale and limestone deposited by transgression and regressions of ancient seas (Hill 1901). Outcropping strata indicate horizontally bedded Cretaceous bedrock slightly

dipping southeast toward the Gulf of Mexico. The Cretaceous bedrock layers are exposed at the surface and due to the dip of the beds, appear in layers trending northeast to southwest. The bedrock outcrop trend is perpendicular to the flow direction of the Brazos River. McLennan County has four geologic groups that underlie the Brazos alluvium: the units are the Woodbine Group, Eagle Ford Group, Austin Chalk, and Taylor Group from the north to the southern border of McLennan County (figure 2). These units act as confining layers below the alluvial sediments, which were deposited on top of the eroded Cretaceous rock.

Since the Pleistocene, sediments have been accumulating in the Brazos River alluvial valley in layered packages (Deussen 1924, Cronin and Wilson 1967). A larger and more competent Brazos River deposited large amounts of commonly siliceous gravels and sands during the early depositional stages (Harlan 1985; Epps 1973). Silt and clay were deposited on top of the sands creating graded packages that fine upward. The river, carrying sediments to the flood plain, also incised earlier deposited layers creating terraces (Stricklin 1961). Lower terraces have been found to be in hydrogeologic communication with the alluvial aquifer and were included as a part of the BRAA (Cronin and Wilson 1967). Harlan (1990) noted the occurrence of increased amount of gravel in the terraces compared to the sand-dominated floodplain. The floodplain alluvium is the dominant water-bearing unit in the BRAA. The alluvial deposits generally become increasingly thicker downstream (Cronin and Wilson 1967). Figure 3 is an exposed gravel wall with in the BRAA illustrating the sediment. The floodplain alluvium is the dominant water-bearing unit in the BRAA. The alluvial

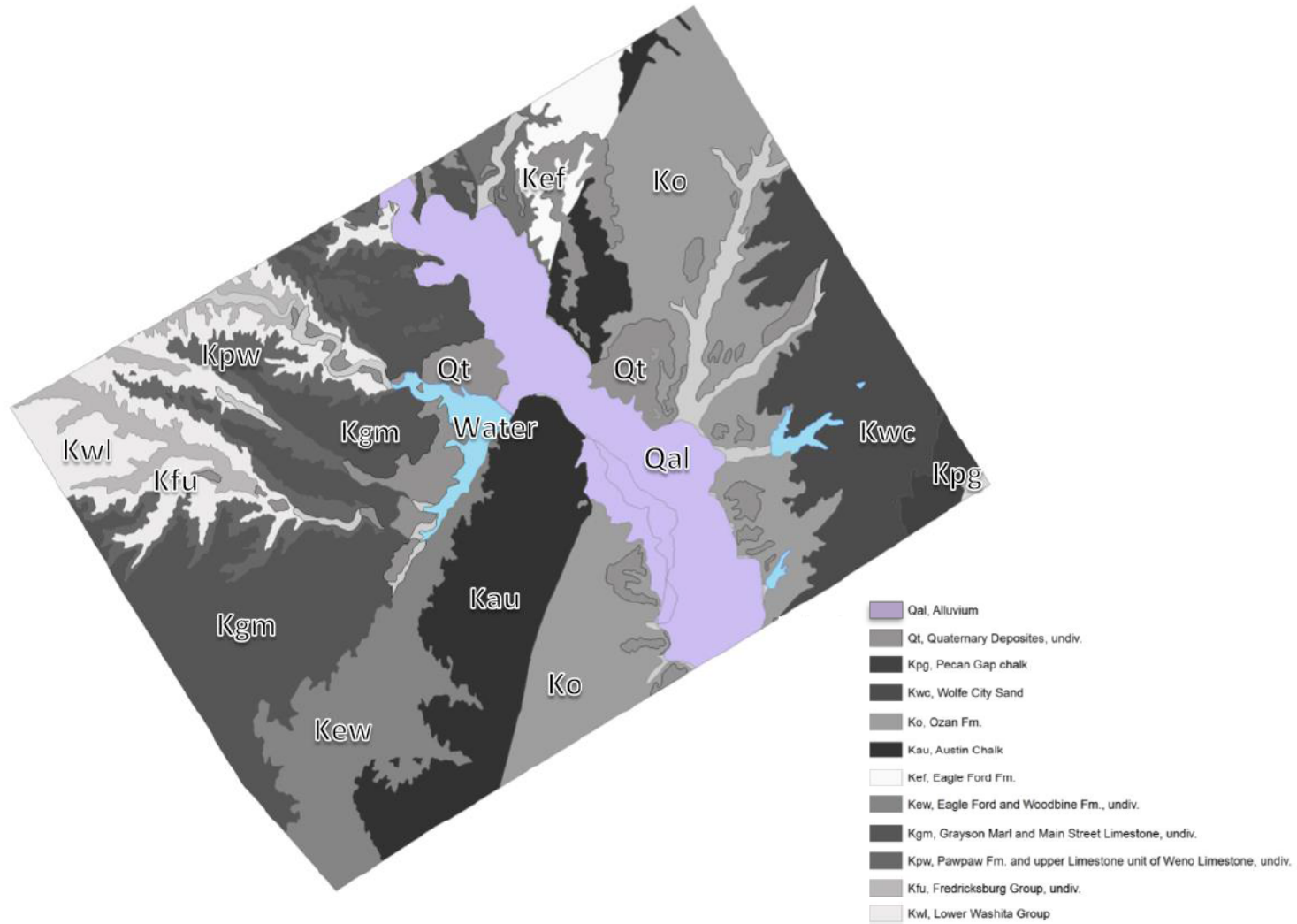


Figure 2. Geologic map labeling major bedrock groups with quaternary-aged alluvial sediment deposited almost perpendicular to bedrock (TWDB)

deposits generally become increasingly thicker downstream (Cronin and Wilson 1967). Figure 3 is an exposed gravel wall within the BRAA illustrating the sediment distribution. The alluvial sediments are poorly sorted but are commonly described as a fining upward carbonate and siliciclastic package. The coarse gravel deposited near the bedrock has high hydraulic conductivity (Cronin and Wilson 1967). Grain size distribution is highly variable on a local basis because of interfingering or pinching out of dissimilar beds (Cronin and Wilson 1967).

### *Hydrogeologic Setting*

Most of what is known about the hydrogeologic parameters of the BRAA can be found in two reports. Cronin and Wilson (1967) of the U.S Geological Survey conducted a study of the hydrogeology of the Brazos River Alluvial Aquifer from Whitney to Richmond, Texas. Shah and Houston (2007) compiled data from previous reports, universities, and groundwater conservation districts to create a GAM-formatted geodatabase. The two hydrogeologic assessments have been summarized in table 1. Wong (2012) filled in sparse data near the southern border McLennan Co. by using well depth to approximate thickness of the BRAA. The alluvium is estimated to be on average 19.5 ft. near McLennan County (Wong 2012) and can range from negligible to over 100 ft. but averages about 50 ft. throughout the entire aquifer (Cronin and Wilson 1967). Harland (1990) studied the groundwater flow of the BRAA near Waco, Texas. He measured water levels in the lower terraces and alluvium and suggested the formations act as a single hydrogeological unit. Groundwater in the BRAA flows toward and discharges into the Brazos River (Scott K. Harlan 1985). It is estimated that the BRAA discharges 2,500 acre-feet per year into the Brazos River. (Yelderman, 2008).



Figure 3. Gravel pit wall showing three distinct layers with in the alluvium. The top consists of light brown soil followed by red to tan fines and coarse material at the bottom

Table 1. Hydrogeologic data of the BRAA found in the literature. Cronin and Wilson 1967 data determined in the laboratory with three different sample collection methods. Shah et. al.

Aquifer Properties	Cronin and Wilson 1967	Shah et all 2007
Hydraulic conductivity (cm/s)	* $4.7 \times 10^{-8}$ – $8.5 \times 10^{-2}$	** $6.3 \times 10^{-2}$ – $1.6 \times 10^{-1}$
Specific Capacity ([gal/min]/ft)	6 - 134	1.44 - 134
Transmissivity (ft <sup>2</sup> /d)	6,684 – 40,104	289 - 27,800
Porosity (%)	24.7-59.5	-

\*Laboratory analysis of Brazos River alluvium floodplain samples

\*\* Hydraulic conductivity derived from seven wells

The groundwater quality of the BRAA has been analyzed by Cronin and Wilson (1967) and Harlan (1990). The baseline chemical analysis of the groundwater found calcium bicarbonate to be the principle waters. Chemically dissimilar waters were attributed to residence time, recharge, mixing, discharge relationships, and land use practices.

## CHAPTER TWO

### Methods

Multiple methods for analyzing samples and data were used to complete this study. Geospatial data were processed using ArcGIS 10. Physical and chemical properties of the aquifer and associated materials were measured using both field and laboratory techniques. Piezometers were installed to aid in resistivity correlation and to perform slug tests, which were compared to published data. These data along with published data were the inputs for a 3D finite-difference model (figure 4).

### *Geospatial*

Spatial data and processing is important in calculating water budgets, creating boundaries for models, and identifying areas of interest. The water budget for the BRAA requires areal measurements of the aquifer, mined pits, and urbanized surfaces to which recharge rates were applied. Published pan evaporation rates corrected with temperature dependent evaporation coefficients were applied to the mined area to estimate total lake evaporation within the study area. Urban surface area were acquired from a 2006 USGS land use map.

Gravel pit model boundaries and were determined by using aerial photographs and GIS software. Excavation sites were distinguished by looking for rows of spoil piles, polygonal dimensions (straight sides), and water-filled pits (Wong 2012). Other boundaries were downloaded from the Texas Water Development Board (TWDB), Texas Natural Resources Information System (TNRIS), and United States Geological Survey.

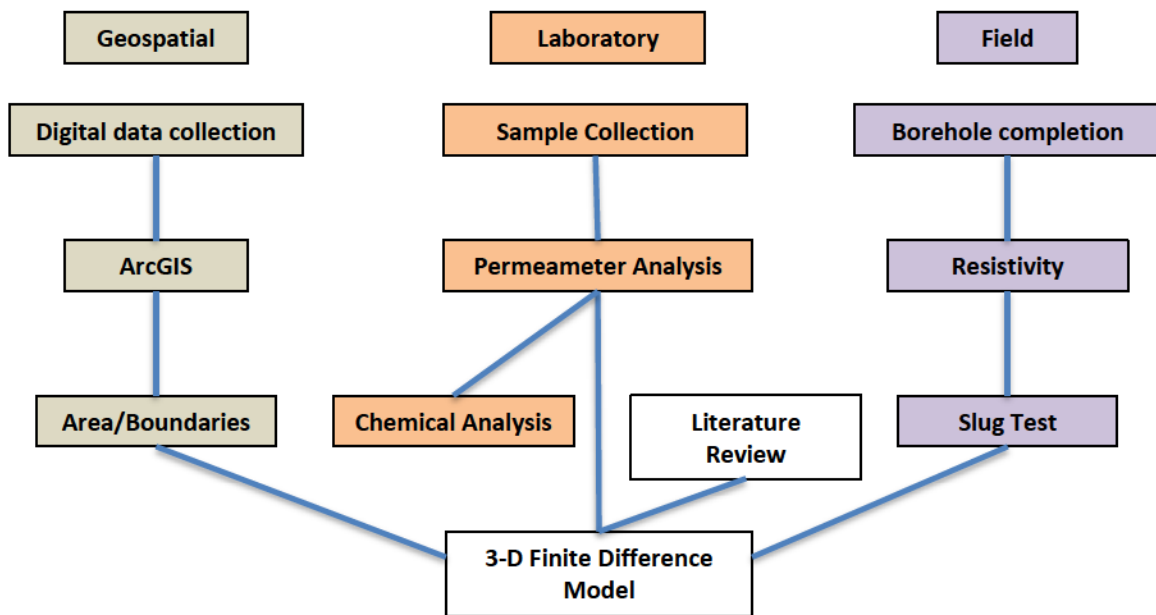


Figure 4. Flow chart illustrating the steps taken in this investigation for Finite modeling inputs.

### *Laboratory*

#### *Permeameter*

Samples were collected from spoil piles, gravel pits, and river cuts. A Modified rigid-wall constant head permeameter measured saturated hydraulic conductivity (K). The permeameter was modified to accommodate large grained sediment and maintain a reasonable representative sample (figure 5). Hydraulic conductivity was calculated using the measured discharge from the permeameter and Darcy's Law (Equation 1).

Porosity (n) was measured by filling the permeameter to the base of the sample and recording the volume it takes to saturate the sample minus the volume of water in the feed tube equal to the length of the sample column. Porosity for fine-grained material was determined by measuring mass (g) and volume (ml). The pore measurements were difficult to determine using the permeameter due to shifting sediment and slow

saturation. A Shelby tube was used to core a volume of material from the permeameter. The tubes and their content were weighed wet and dry. Porosity was calculated by one minus the quotient of bulk density over the particle density (Brandy 2008) (equation 2).



Figure 5. Modified large bucket permeameter. Samples were loaded into the sample chamber. Hydraulic head was kept constant in the constant head regulator with an overflow return

### Equation 1

#### 1.1 Darcy's Equation

$$Q = K I A$$

Q = discharge (cm<sup>3</sup>/s), K = hydraulic conductivity (cm/s), I (dh/dl) = hydraulic gradient, A = Area (cm<sup>2</sup>)

#### 1.2 Darcy's Equation arranged to solve for Hydraulic Conductivity

$$K = (V L) / (A T h)$$

K = hydraulic conductivity (cm/s), L = length of column (cm), V = Volume (cm<sup>3</sup>), A = Area (cm<sup>2</sup>), T = time (s), h = head (cm)

### Equation 2

$$\text{Porosity (n)} = 1 - D_b / D_p$$

D<sub>p</sub> (particle density) = Mass of dry sediment / volume of solids, D<sub>b</sub> (bulk density) = mass of dry sediment/total volume (solids and pore spaces)

The permeameter had minor leaking in the pvc fixtures, addressed with sealing compound, and sidewall. The large-scale bucket permeameter design was used to compensate for large grain size and sidewall issues. The sidewall issue remained and appeared to be more prominent in tight samples. The unconsolidated samples were poured into the sample chamber of the permeameter to simulate infilling. The randomness in the orientation of large grains made it difficult to maintain a seal on the walls of the permeameter. Sample packing was left to a bare minimum to maintain and recreate the filling method of real pits.

### *Chemical Analysis*

Tap water from the City of Waco, TX. was the electrolyte used to derive water chemistry from the field samples. The electrolyte was calcium bicarbonate rich water similar to the groundwater of the BRAA (Cronin and Wilson 1976). Percolated water samples from the permeameter were measured for temperature, hydraulic conductance, and pH using probes. Exposure time for the water to react with the samples was dependent on the permeability and column length. Controlled batch leaching allowed equal water rock exposure time for anions and cations to reach equilibrium. The batch equilibration method consists of mixing a sample with a known amount of electrolyte solution, agitating the container until combined, and storing in a temperature controlled environment (Dibonito and others 2008). The batch method is also a common laboratory method used in contaminated site studies and for predicting the chemical behavior in soils. Bicarbonate concentrations were determined with acid titration. The water samples were analyzed for common cations (Ca, Na, K, Mg,  $\text{HCO}_3$ ) and anions ( $\text{SO}_4$ , Cl, N, F,

PO<sub>4</sub>) using a Quanta 4000 electrophoresis capillary. Accuracy of the analysis was tested with three standards.

The fresh concrete and brick samples were rewetted for 48 hours and again for two months for a short term and long-term leaching to examine the potency of fresh material over time. The saturation period of the second exposure was the same as the first exposure allowing ample time to equilibrate to the initial reading.

### *Field*

#### *Resistivity*

Two-dimensional direct-current resistivity is a commonly used method for interpreting depth and lateral extent of sediment, depth to bedrock, and depth to groundwater (Shah and others 2007; Zohdy and others 1974). The surveys were conducted using a SuperSting R8 IP meter and four 13-node electrodes spaced two meters apart (figure 6). The distance between electrodes totaled 110m allowing for penetration depth of 25m. Dipole-dipole array was used to measure the subsurface distribution of electrical properties. A detailed explanation of the dipole-dipole resistivity survey method is thoroughly outlined by Zohdy and others (1974). The dipole-dipole array is capable of yielding high-resolution horizontal data sets and mapping vertical structures (Loke, 2004). Shah and others (2007) have illustrated the application of inverse modeling methods used in resistivity investigations. The inverse modeling was conducted using EarthImager 2D software.

### *Borehole*

Boreholes were drilled to install piezometers and ground truth the geophysical data (figure 7). Bore holes cuttings were logged and superimposed onto the 2D resistivity profiles. The bottom of the boreholes was drilled to a depth where a clay-rich unit occurred and believed to be the confining shale unit. The piezometers allowed for water table and hydraulic conductivity measurements. Slug tests were conducted on the Hirsh Dairy wells using 5 gallons of water as the slug and a level logger to collect the water level change over time.

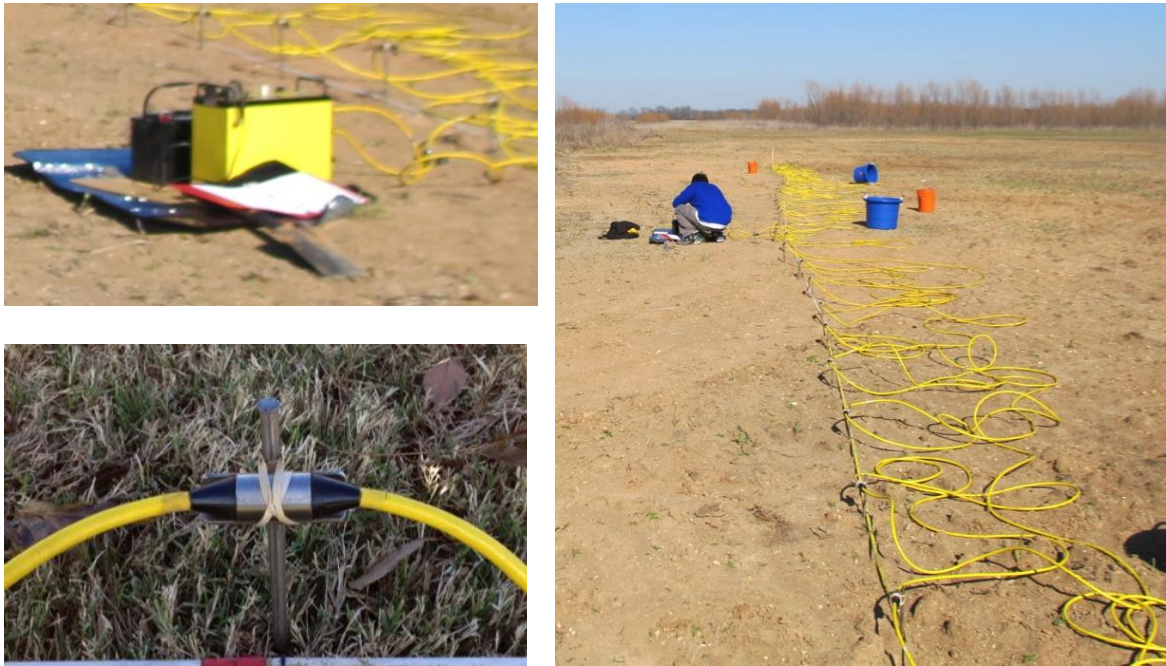


Figure 6. Resistivity survey in the field. The yellow box is the SuperSting R8 IP meter. The yellow cables plug into the SuperSting and couple to steel spikes staked into the ground.



Figure 7. Drill rig with four inch auger stem drill. Boreholes were completed as screened piezometers.

### *Finite Difference Modeling*

A portion of the BRAA containing several gravel mine open pits was modeled using Model Muse to compare effects from several hypothetical situations related to aquifer restoration. Model Muse is an object oriented graphical pre and post processor that allows users to set up the boundaries and conditions for a groundwater model before processing the data through MODFLOW 2005 finite difference groundwater model source code (Harbaugh 2005; M.G. and A.W. Harbaugh 1988; Winston 2009). MODFLOW 2005 outputs were post processed in Model Muse using MODPATH 5.0 to track particle motion in the simulated aquifer (Pollock 1994). The BRAA was modeled in steady state to calibrate the head levels and to create baseline head data.

MODFLOW Packages and environmental inputs:

- No flow boundaries were assigned to all cells outside of the modeled area.
- MODFLOW's River Package interpolated a river gradient and assigned a free water surface one meter higher than the streambed surface elevation.
- MODFLOW's Recharge Package was used to simulate aerial recharge to the aquifer. An estimated four percent of precipitation, based on HDR Engineering Inc. 2001, was later reduced to two percent
- MODFLOW's Well Package was used to inject water from the west boundary to simulate groundwater contribution.
- MODFLOW's Evapotranspiration Package was used to simulate lake evaporation.

## CHAPTER THREE

### Results and Discussion

#### *Geospatial*

The boundary of the BRAA is estimated to include 154 mi<sup>2</sup> (figure 8). Mined areas and urbanized surfaces affect about 22 mi<sup>2</sup> of the aquifer, about 14.5%. Of the affected area, urbanized surfaces account for 16 mi<sup>2</sup> (10%) with the remaining 6.8 mi.<sup>2</sup> (4.4%) occupied by sand and gravel operations (figure 8). The remaining 132 mi<sup>2</sup> (85.5%) of the aquifer were considered undisturbed aquifer.

The boundary for the aquifer was modified to include portions of lower terrace, south of Waco, TX. The lower terraces are in hydraulic communication with the aquifer. The hydraulic connection was observed in groundwater filled mined areas outside of the previously established aquifer boundary. Estimation of urban cover was concentrated around the most heavily urbanized areas and included green space within the identified urban area, which can lead to an over estimation. Exclusion of isolated structures, some rural communities, and external roadways in the non-urban area may offset some of the over estimation in urban area. Mining area estimates were calculated from recent aerial photographs, 2003 to 2010. Gravel mining operations can have operating durations less than the frequency in which aerial photographs are taken thereby limiting the ability to account for all mining activity within the BRAA using aerial photographs for identification.

Recharge to the BRAA was calculated using the thirty-seven year average precipitation rate of McLennan County or 33.9 inches (0.861 m) (figure 9). Lake

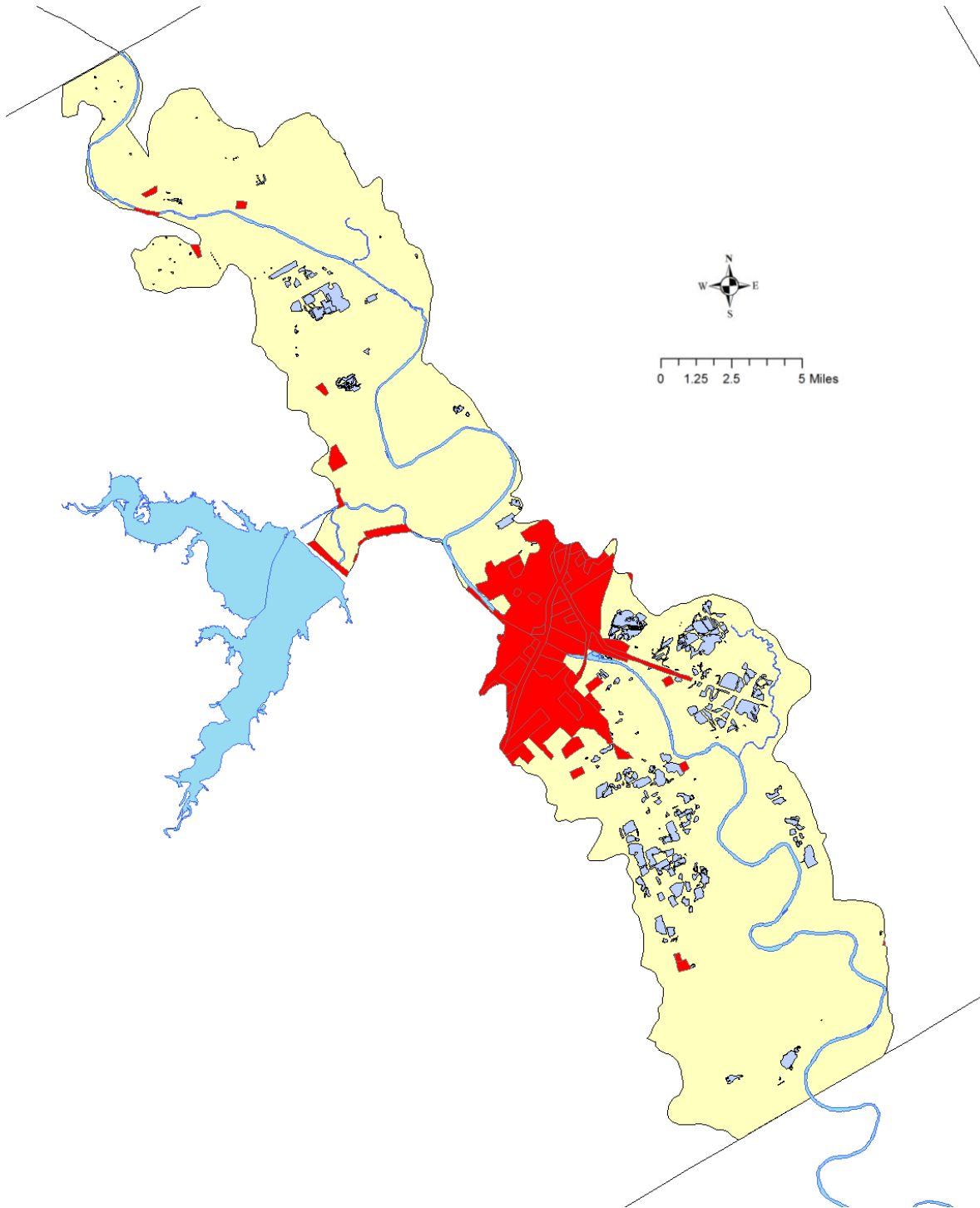


Figure 8. Spatial analysis of the BRAA. The yellow area represents un-disturbed aquifer, the gray is mining activity, and the red is urbanized cover.

evaporation was calculated from published pan evaporation rates (60 in) corrected with the average lake evaporation coefficient of 0.7 for this area. Different amounts of

recharge were applied to undisturbed aquifer zones, mined areas, and urban areas (table 2). The undisturbed aquifer recharge zone received 7.5% (Cronin and Wilson 1967) of the precipitation totaling 18,381 acre-feet in the BRAA. Urban surfaces were considered impermeable diverting 2,157 acre-feet of annual rainfall away from recharge zones. Mined areas recharge the groundwater directly and collect 100% of the precipitation received totaling 12,528 acre-feet to the annual budget. Lake evaporation in mined areas removes 15,120 acre-feet of groundwater resulting in a net loss in the groundwater budget of 2,592 acre-feet (12%) and an annual recharge of 15,789 acre-feet.

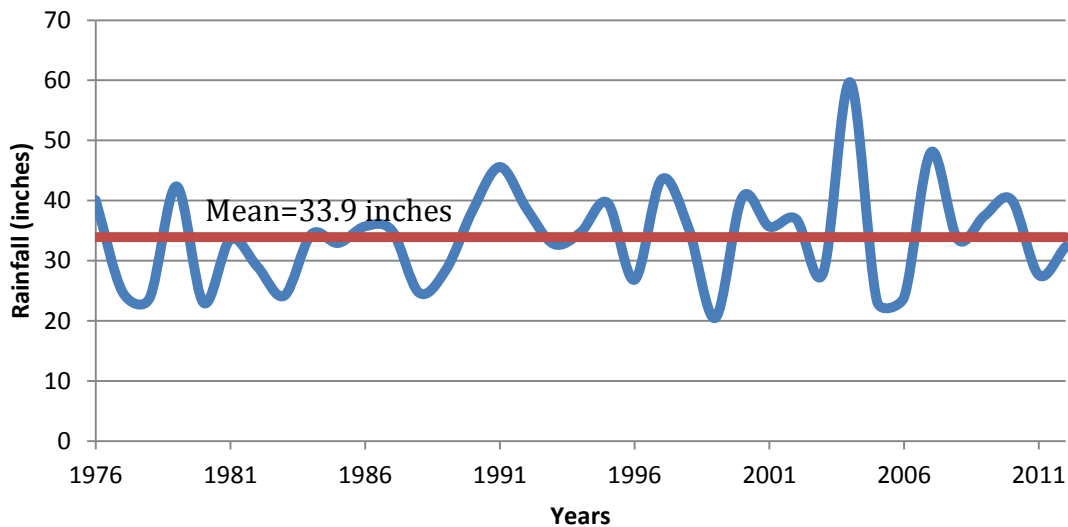


Figure 9. Annual rainfall for Waco, Texas from 1976-2012. Mean annual rainfall over a 37 year period is 33.9 inches (0.86 meters). Data collected from Texas Water Development Board (TWDB).

Similarly, the Texas Water Development Board (TWDB) determined the Managed Available Groundwater (MAG) for the portion of the BRAA to be 15,023 acre-feet per year of which 14,448 acre-feet is annual recharge. The discrepancy between the MAG recharge and the calculated 15,789 acre-feet estimate comes from the aquifer boundary modification. Cronin and Wilson’s (1967) 7.5% recharge rate, used to estimate recharge

on the unaltered zone, was found to be high and model to be about 4% by HDR Engineering (2001). The HDR reduction in recharge rate decreased the aquifer recharge to 9,803 acre-feet and the total recharge to 7,211 acre-feet (table 2). Using a dated recharge rate may be a large oversight in budgeting groundwater resources. More recent studies along with modeling techniques can be used to more accurately calculate available groundwater.

Table 2. Recharge estimation for the BRAA with in McLennan County. Spatial data collected in ArcGIS, Recharge rates from literature, and mean annual climate data from NOAA and TWDB.

Total Aquifer Area	98,752 acres	
- Mining and Urban Area	14,240 acres	
	Unaltered Aquifer	84,512 acres
x Average Precipitation	2.9 ft.	
x Recharge Factor*	.075	.04
	Recharge to aquifer	18,381 acre-feet
+ direct recharge into Pits		9,803 acre-feet
		12,528 acre-feet
	Total recharge	30,909 acre-feet
- Gravel Pit area	4320 acre	
Evaporation	5 ft.	
Lake evaporation factor	7	
Evaporation Lost from Mined areas	15,120 Acre-feet	
Remaining Recharge	15,789 acre-feet	7,211 acre-feet

Mined surfaces account for a small fraction of the aquifer area but a disproportionately large decrease in recharge. Depending on the infiltration rate used, the water budget is reduced by twelve to twenty three percent compared to non-mining

conditions. The percent recharge lost to percent mined area ratio is 2.74 meaning for every percent increase in mining area that exposes the groundwater, the equivalent of 2.72 percent of annual recharge is lost. If mining areas continue to be exposed to evaporation, future mining will further decrease the water budget.

Based on the observation that most mined areas have exposed water surfaces, water budget calculations were simplified by assuming all mined areas to have exposed water surfaces. Addition of the filled areas without exposed water did not greatly change the calculations.

Urbanized surfaces cover about a tenth of the aquifer and were estimated to reduce the recharge by about ten percent. Urban areas effectively decrease the recharge equivalent to undisturbed aquifer recharge of equal size. This is true under the assumption that urbanized surfaces are completely impermeable. The addition of urban surfaces was added to the recharge calculation because of its large presence in the aquifer. The impermeability assumption was made to simplify calculations. Many factors of urbanization such as pumpage, irrigation, leakage from pipes, and secondary fracture porosity have been studied to create fluctuations in the water budget in the urban environment (Hibbs and Sharp 2012; Passarello, Sharp, and Pierce 2012). The oversimplification of urbanization as an impermeable surface does not characterize all potential impacts on the hydrogeology. Further investigation should be conducted on urban effects.

In terms of well installation and production ability, unaltered-aquifer areas offer the most potential for permitted well construction. Mined areas have no aquifer framework or overburden making it difficult to construct a well. Urban areas have paved

surfaces, buildings and land use restrictions, such as cemeteries, that inhibit drilling and production potential. With mined areas exposing groundwater to evaporation and drastically affecting the water budget, studying the properties of fill materials and their effect on the aquifer could be useful.

### *Laboratory*

#### *Sample Collection and Description*

The collection of aquifer material, native fill material, and foreign materials in the field were clustered near currently abundant gravel pits (figure 10). The majority of the samples were collected from the most heavily mined area, south of Waco, TX. The sample taken north of Waco, TX. is owned by a construction company excavating for sand, gravel, fill dirt, and top soil. Aquifer materials were collected along pit walls and river cuts, or taken from freshly excavated gravel piles (figure 11c). Native material was collected from overburden piles lining the outer perimeter of the pits. Foreign material was collected from pits, low areas, and construction sites.

The number and distribution of samples collected is not a perfect representation of mining in the BRAA. Collection was limited by accessibility, landowner permission, and clast size. Native material proved to be the most accessible, which may be due to the lack of infilling and abundance of overburden berms (figure 11b). Foreign materials are abundant in the field but more difficulty was experienced with sampling them. These materials were often found in mined areas rather than around them. Foreign materials were identified in the field by dissimilar features like color, lithology, and the addition of

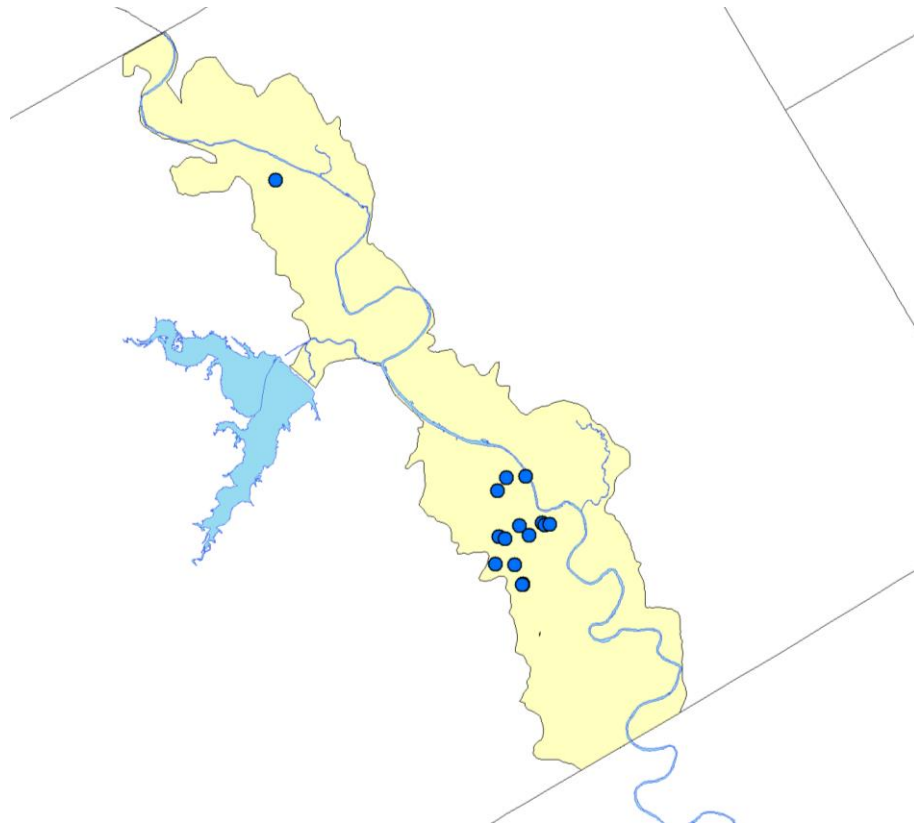


Figure 10 Field sample collection locations. The samples were collected for laboratory testing. There are 16 total samples. Some samples were collected in close proximity to each other and may be harder to distinguish on the map.

anthropogenic materials (figure 11a). Foreign materials with similar features as the alluvium might be missed. Some large clasts, twenty-five centimeters or above, were observed at most foreign material sample sites but could not be collected practically.

The most challenging material to sample was the aquifer material. BRAA sand and gravel is often excavated then quickly sorted and sold leaving little opportunity to sample. Also, gaining access to gravel pits has safety concerns associated with it and permission was difficult to obtain. Samples of the different materials are shown and described in figure 12 and figure 13. Foreign materials contain highly variable and



Figure 11. Examples of collection sites. a. Spoil pile containing anthropogenic materials. b. Overburden spoil piles native to the mining area. c. Pile of excavated aquifer material and (d.) a river cut.

dissimilar characteristics among samples. A second level of classification split foreign materials into natural foreign material and anthropogenic material (figure 13). The anthropogenic material classification descriptions were kept general in order to group and point out the dominant grain types specific to the BRAA. Grains can drastically change in size, shape, and material due to variables such as location, culture, land use, etc.

The aquifer materials were described as consisting of varying amounts of mostly gravel, sand, and fines (figure 12). Gravely sand provides some of the best porosity and permeability for groundwater production but is susceptible to production declines as the amount of fines increases. Representative heterogeneity of the BRAA is not well reflected in the samples because collection sites were predominantly from mining operations that target the sand and gravel. No aquifer material samples represented clay lenses or large amounts of silt present in the BRAA. Permeability on aquifer samples is viewed as a high estimate compared to the overall BRAA because sample locations were in economically targeted gravel deposits.

Native materials were described as mostly clay and silt (figure 12). Few samples included poorly developed soil containing organics. The most noticeable feature, in regard to infilling mines, was the structures of the disturbed overburden. The ripped up fine material harden into clasts developing a secondary structure. The native material clasts ranged from coarse sand to gravel sized.

The Austin Chalk was the only natural foreign material collected. The chalk was being used to fill a depression in a field. Although the chalk collected was not occupying a mined area, it represents local natural fill. Anthropogenic-sourced foreign materials are



*Aquifer Material*

Alluvial deposit, tan to reddish orange to grey. May contain calcareous gravel, silica sand, and fines. Grains range from clay to gravel (7mm), poor to moderately poor sorting, sub angular to round grains.



*Native Material*

Alluvial soil, tan to reddish brown to black. May contain clay, silt, with lesser amounts of sand and rarely gravel. Grass, roots, other biota are present. Secondary structures were present as ripped up clay hardened to clasts.

Figure 12. General description of aquifer material and native material with pictures

dominated by building materials (figure 13). Concrete, bricks, and asphalt are common clasts observed. Construction related materials like rebar, corrugated metal, pipes, wire, etc. were less abundant. Large clasts were mostly angular and poorly sorted. The pore spaces created by the large clasts were often filled with fine particles of similar material.



*Natural Foreign Material*  
Grains range from clay to > 25mm.  
Greater than 50 mm clasts were  
observed in uncollected field grains.  
Poorly sorted, rounded to angular.  
Carbonate rich



*Anthropogenic Material*  
Grains range from clay to > 25mm.  
Greater than 50 mm clasts were  
observed in uncollected field grains.  
Poorly sorted, rounded to angular.  
Clay and silt matrix contains organics.  
Larger grains include asphalt, wire,  
construction equipment, corrugated  
metal pipe (CMP), bricks, concrete,  
and mortar.

Figure 13 Description of foreign materials sub-divided into natural foreign materials and anthropogenic materials

### *Permeameter Data*

The permeameter data are shown in figure 14 and table 3. The aquifer samples ranged from  $2.7 \times 10^{-3}$  cm/s to  $2.6 \times 10^{-2}$  cm/s and averaged  $1.8 \times 10^{-2}$  cm/s. The native fill had the largest hydraulic conductivity range from  $6.7 \times 10^{-5}$  cm/s to  $1.8 \times 10^{-2}$  cm/s and averaged  $5.1 \times 10^{-3}$  cm/s. The hydraulic conductivity of foreign fill occurs in the upper ranges, from  $6.9 \times 10^{-3}$  cm/s to  $5.1 \times 10^{-1}$  cm/s, with a mean average of  $2.3 \times 10^{-1}$  cm/s. The porosity values varied depending upon the material. The clay and silt rich samples had the highest percentage of pore space compared to the coarser sand and gravel rich materials (appendix A).

Native fill material had the widest range in hydraulic conductivity. Well-developed clay layers generally act as aquitards and have low permeability but ripped up and reworked clays respond differently. Samples with the lowest measured K were clay-rich and swelled when hydrated. Higher K samples either consisted of silt and sand or the result of the formation of clasts. The unusually high K measurement of some clay-rich samples could be explained by a number of factors but observation of hard clasts being slow to hydrate and retaining their secondary structure, after multiple pore volumes, suggests increased pore size as the most likely mechanism. Small amounts of sand and gravel, present in many of the samples, did not greatly influence permeability.

Foreign materials had the highest hydraulic conductivity values. The abundance of large irregularly shaped clasts with poor granular packing allowed macro pores to develop in these highly permeable samples. The permeability created by these macro pores was inhibited by the fine-grained sediment but often bypassed with high K preferential pathways. The short duration of the experiment did not explore sediment

accumulation in macro pores over time. The less permeable foreign materials had much higher amounts of fine material associated with them.

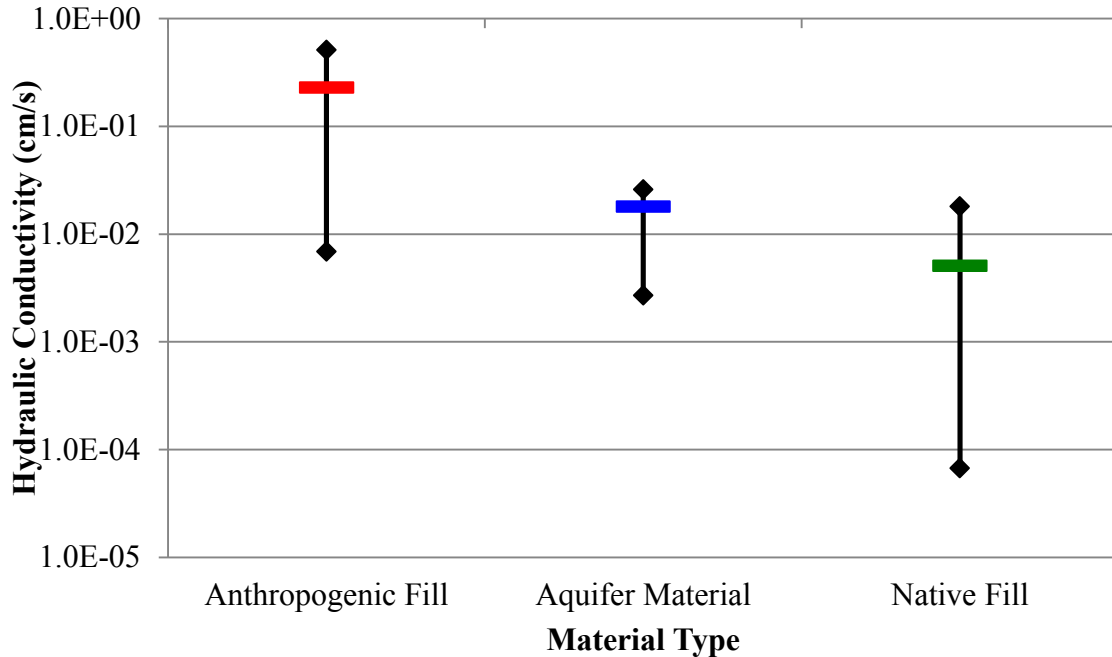


Figure 14. Hydraulic conductivity of unconsolidated material using a modified constant-head bucket permeameter. Maximum, mean, and minimum values are plotted for each material group.

Table 3. Average hydraulic conductivity for samples

Aquifer Material	K (cm/s)	Native Fill	K (cm/s)	Anthropogenic Fill	K (cm/s)
<b>Brazos sand</b>	1.8x10 <sup>-2</sup>	<b>For Sale</b>	1.8x10 <sup>-2</sup>	<b>Austin Chalk</b>	5.0x10 <sup>-1</sup>
<b>Rosenfeld sand</b>	2.5x10 <sup>-2</sup>	<b>New Pit</b>	1.0x10 <sup>-2</sup>	<b>Equestrian Site</b>	6.9x10 <sup>-3</sup>
<b>Kuntz</b>	2.7x10 <sup>-3</sup>	<b>Rosenfeld</b>	4.3x10 <sup>-4</sup>	<b>Lockwood Lane</b>	1.1x10 <sup>-1</sup>
<b>Hirsh Dairy</b>	2.6x10 <sup>-2</sup>	<b>Tan Pit</b>	1.8x10 <sup>-3</sup>	<b>Rosenfeld Fill</b>	5.1x10 <sup>-1</sup>
<b>Horseshoe Bend</b>	2.0x10 <sup>-2</sup>	<b>Locked Gate</b>	6.7x10 <sup>-5</sup>	<b>Hirsh Dairy Fill</b>	8.3x10 <sup>-3</sup>
		<b>Hirsh Dairy</b>	3.9x10 <sup>-4</sup>		
<b>Max</b>	2.6x10 <sup>-2</sup>	<b>Max</b>	1.8x10 <sup>-2</sup>	<b>Max</b>	5.1x10 <sup>-1</sup>
<b>mean</b>	1.8x10 <sup>-2</sup>	<b>mean</b>	5.1x10 <sup>-3</sup>	<b>mean</b>	2.3x10 <sup>-1</sup>
<b>min</b>	2.7x10 <sup>-3</sup>	<b>min</b>	6.7x10 <sup>-5</sup>	<b>min</b>	6.9x10 <sup>-3</sup>

Aquifer material had the least amount of K variation ranging approximately one order of magnitude. The measured mean K was  $1.8 \times 10^{-2}$  cm/s. Published data ranged from  $4.7 \times 10^{-8}$  cm/s to  $1.6 \times 10^{-1}$  cm/s and averaged  $8.5 \times 10^{-2}$  cm/s as a mean (J. Cronin and Wilson 1967). The aquifer materials analyzed through the modified permeameter were economically targeted gravels and sands from mining operations, which may have contributed to a higher estimate. These sands and gravels are representative of high production zones within the BRAA and do not typify the entire aquifer. Permeability outside of the mined area was measured with well tests.

Bouwer and Rice (1976) slug tests, performed on two wells in the BRAA, measured an average permeability of  $8.0 \times 10^{-4}$  cm/s, almost two orders of magnitude less than permeameter estimates (appendix B). Borehole logs show mostly fine grained materials in the well suggesting a lower production zone of the aquifer and material more similar to native material (appendix B).

Permeability within the BRAA is as variable as the materials found filling mined areas but the pre-mining K of mined areas may have a narrower permeability range compared to the BRAA. Aquifer material found at gravel mines had higher K compared to measurements outside of mined areas. High-K aquifer material at mined areas suggests that fill material should have similar permeability values in order to allow for groundwater to flow naturally.

### *Chemical Analysis*

Water samples were initially tested for pH and electrical conductivity (Ec). Most samples fell within a pH range of 7.2 to 8.3 and Ec range of 315 to almost 500 $\mu$ S. Measurements exceeding these ranges were mostly associated with foreign fill. Fresh

concrete and bricks collected from a building demolition was also tested to compare water chemistry of fresh material to weathered material collected from the field. Bricks exhibited a normal pH range but had high Ec topping out at 1850  $\mu\text{S}$ . Concrete had pH readings ranging 8.8 – 9.3 and Ec from 1323 – 3750  $\mu\text{S}$  (table 4).

All samples with pH reading at 8 or higher, except for the Locked Gate sample, were collected from currently operating mine or had substantial amounts of concrete incorporated in the sample. Although the pH levels were within the normal range observed in the BRAA, mining activity and reworked material were thought to be factors in increasing pH of native and aquifer materials. Increased pH or Ec in water samples containing anthropogenic material is strongly influenced by the presence of high pH concrete. The Equestrian Site sample was collected near a horse corral and exhibited high Ec while maintaining a neutral pH. In contrast, a concrete dominant sample recorded Ec levels similar to aquifer material but a pH measurement comparable to fresh concrete material.

Major ion chemistry provided in table 4 was plotted on a piper diagram (figure 15). The waters derived from aquifer and native material were calcium bicarbonate rich with the exception of one native sample with high sodium concentration (figure 15). The majority of aquifer samples show a detectable level of nitrate that was not present in the electrolyte. Nitrate was less common in the native material water samples. The aquifer material and native material water chemistry had similar proportions of ions.

The chemical analyses of the waters sampled in the BRAA are comparable with previous studies in this area. Harland (1990) and Cronin and Wilson (1967) provide baseline chemical data for the BRAA (appendix C). Aquifer sample and native sample

Table 4. Ionic concentrations given in mg/l, pH, and Ec ( $\mu$ S). Phosphate and fluoride (not plotted) were not detected in any samples.

Sample	Cl <sup>+</sup>	SO <sub>4</sub> <sup>2-</sup>	N <sup>+</sup>	K <sup>+</sup>	Ca <sup>2+</sup>	Na <sup>+</sup>	Mg <sup>2+</sup>	HCO <sub>3</sub> <sup>2-</sup>	ph	Ec
Tap water	25.78	25.81	0	4.48	40.47	17.48	4.82	141.98	7.3	330
Aquifer	Cl <sup>+</sup>	SO <sub>4</sub> <sup>2-</sup>	N <sup>+</sup>	K <sup>+</sup>	Ca <sup>2+</sup>	Na <sup>+</sup>	Mg <sup>2+</sup>	HCO <sub>3</sub> <sup>2-</sup>	ph	Ec
Brazos sand	52.27	42.32	17.97	0	68.64	20.63	6.16	146.88	7.3	474
Rosenfeld sand	34.56	37.25	29.86	0	58.51	20.47	5.72	171.36	7.3	420
Kuntz aquifer	61.61	28.73	0	0	127.00	43.41	6.39	181.15	7.5	488
Hirsh aq	31.37	59.56	23.29	0	71.95	14.61	1.12	110.16	8.1	370
horseshoe	29.12	26.40	28.45	0	62.88	14.87	2.03	116.28	8.1	315
Foreign	Cl <sup>+</sup>	SO <sub>4</sub> <sup>2-</sup>	N <sup>+</sup>	K <sup>+</sup>	Ca <sup>2+</sup>	Na <sup>+</sup>	Mg <sup>2+</sup>	HCO <sub>3</sub> <sup>2-</sup>	ph	Ec
Austin Chalk	35.79	31.35	30.22	0.47	68.44	18.23	2.762	117.50	7.2	386
Equestrian Site	70.81	66.23	114.00	88.48	113.10	18.16	11.42	201.96	7.2	854
Lockwood lane	27.92	114.20	0	5.83	53.15	41.70	0	85.68	9.1	427
Rosenfeld Fill	37.63	153.90	0	2.63	115.10	16.79	4.12	85.68	8.1	572
Hirsh anthro	52.90	142.70	12.70	0.11	79.26	45.89	7.65	73.44	8	638
Native	Cl <sup>+</sup>	SO <sub>4</sub> <sup>2-</sup>	N <sup>+</sup>	K <sup>+</sup>	Ca <sup>2+</sup>	Na <sup>+</sup>	Mg <sup>2+</sup>	HCO <sub>3</sub> <sup>2-</sup>	ph	Ec
For sale	37.24	25.98	0	0.59	63.22	18.46	1.86	117.50	7.6	326
New Pit	53.35	27.29	0	0	44.31	35.83	5.98	140.76	7.6	355
Rosenfeld soil	35.02	34.94	13.76	0	84.52	22.27	3.62	159.12	7.4	432
Tan pit	33.34	30.91	0	0	65.54	18.01	2.59	129.74	7.4	351
Hirsh native	1.62	39.78	40.68	0	52.80	19.51	3.86	122.40	8.3	355
Locked Gate	66.82	41.55	0	0	21.90	71.34	5.55	261.94	8.1	602
Other	Cl <sup>+</sup>	SO <sub>4</sub> <sup>2-</sup>	N <sup>+</sup>	K <sup>+</sup>	Ca <sup>2+</sup>	Na <sup>+</sup>	Mg <sup>2+</sup>	HCO <sub>3</sub> <sup>2-</sup>	ph	Ec
Concrete	128.8	2227.00	0	46.80	345.50	95.28	423.40	15.91	8.8	3750
concrete 2nd	58.81	775.50	0	52.81	145.30	71.38	79.88	15.91		1323
concrete 3rd	58.92	1286.00	42.19	56.51	497.80	96.22	16.41	24.48	9.3	2100
brick	124.70	530.60	131.30	24.41	276.60	90.72	28.32	283.97	7.4	1850
Brick 2nd	63.57	161.20	0	25.61	135.50	68.47	13.12	283.97		703
brick 3rd	48.30	247.40	20.91	14.14	176.00	32.5	15.63	226.44	7.7	938

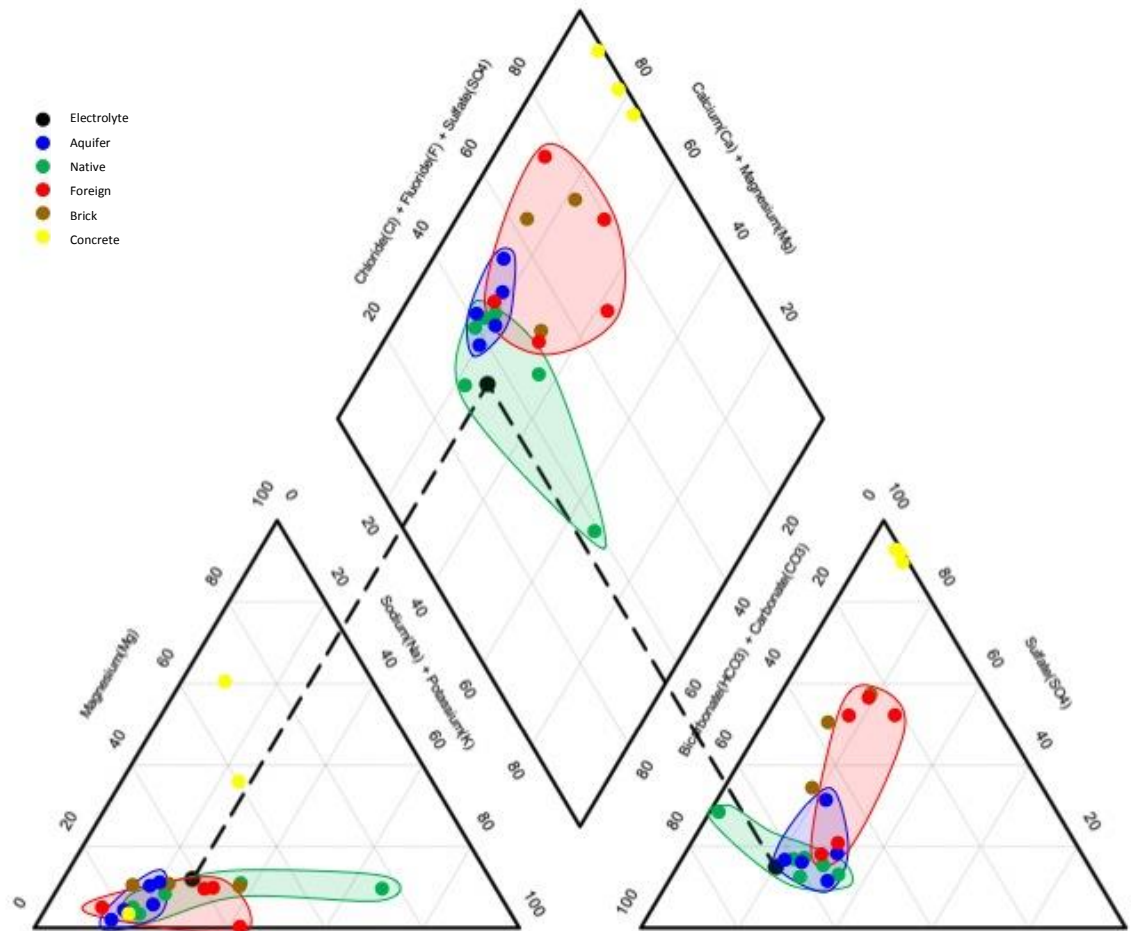


Figure 15. Piper diagram to determining water type. A shape was drawn around the aquifer, native and foreign materials to show the range of chemistry. The Brick (brown) and concrete (yellow) have only one sample each but were leached multiple times.

waters were within the normal chemical range expected from the groundwater analyzed from the BRAA (appendix C). The narrow range of concentration analyzed by this study is due to the small sample size. Aquifer and native fill material were deposited in the same environment and are lithologically similar. It is reasonable to expect the water derived from these two materials be similar.

The water derived from foreign material had calcium as the dominant cation but grouped into two types of water separated by the anion species, bicarbonate and sulfate type (figure 15). The natural foreign material (chalk) and the Equestrian Site sample were bicarbonate dominant, similar to aquifer material and native material respectively (figure 15). The samples containing concrete plotted as sulfate type waters (figure 15). The anthropogenic foreign material samples had increased sulfates and decreased bicarbonate concentrations when concrete was present (table 4). Fresh concrete had the most sulfates and the least bicarbonate of all samples (table 4).

Fresh concrete and brick had large fluctuations in many of the parameters measured (table 4). The 48-hour batch resulted in greater than 50% drop in Ec. The two-month batch saw a drop from the initial Ec by less than half. The 48-hour batch demonstrated the ability for Ec levels to quickly decrease substantially with a second exposure, while the two-month batch showed an overall decrease over time. Shorter saturation period of the second exposure could explain the Ec rebound observed in the third exposure.

Fresh concrete and brick response to multiple exposures was used to observe the chemical potency as the material weathers reflected by ion concentration fluctuations. Ions that followed the Ec fluctuation pattern for concrete were sulfate and to a lesser

extent calcium and sodium. Magnesium levels dropped from 432 to 16 mg/l, potassium increased steadily, and bicarbonate remained at low concentrations (figure 16). For fresh brick, sulfate, calcium, and magnesium followed the Ec pattern. Potassium concentrations were low and decreased slightly, sodium had a constant decline, and bicarbonate maintained high concentrations with some decrease in exposure three (figure 16).

The natural foreign chalk material yielded waters similar to aquifer and native material because the material is carbonate rich and naturally part of the BRAA. Foreign Equestrian sample plotted similar to native material and one of the brick extractions because the material was composed of mainly fine material and bricks. The sample is also rich in potassium and nitrate, attributed to the close proximity to a horse corral. Asphalt was present in the sample but treated as inert at this point. The compounds to interpret asphalt interactions were not tested. The anthropogenic foreign materials were interpreted to have been influenced by concrete. Low  $\text{HCO}_3$  and increased  $\text{SO}_4$  concentrations of fresh concrete material were observed in foreign materials collected in the field, contradictory to what is normally observed waters in the BRAA.

One reason for the switch in the dominant anion and cation over time is the dissolution of concrete particles. Gypsum (calcium sulfate) is often blended in concrete as an additive along with fly ash and other sources of sulfates (Barbudo et al. 2012). The exposure of concrete to water allow for reactions with highly soluble sulfate (Glasser and others 2008). Over time concrete particles on the surface dissolve and the surfaces of the larger concrete clasts diminish the amount of soluble sulfates.

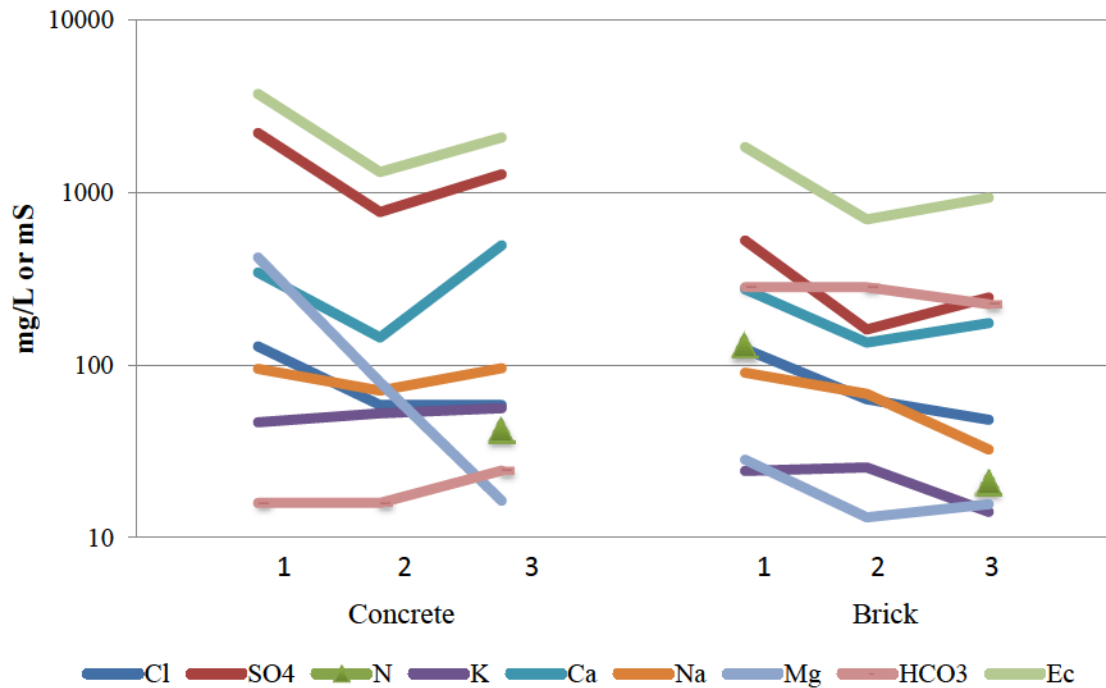


Figure 16. Concentration fluctuations of fresh concrete and brick material over three exposures. 1<sup>st</sup> exposure is 48 hours, 2<sup>nd</sup> exposure in 48 hours, and 3<sup>rd</sup> exposure is two months.

The addition of concrete and brick to the aquifer framework is a concern because of their tendency to readily dissolve and release ions into the water. There is some promise for the use of building materials to safely fill open pits. The breakdown of concrete over time was observed to significantly reduce almost all ionic concentrations with short residence time and over a longer term reduce sulfate concentrations and increase bicarbonate concentrations. Using the more conservative long-term rate, concrete 1<sup>st</sup> and concrete 3<sup>rd</sup>, and the Rosenfeld concrete sample as the weathered end member, the slopes suggests concrete dissolution from fresh concrete to weathered concentrations in as little as four months (figure 17). The  $R^2$  for Ec, sulfate and bicarbonate are 0.999, 0.997, and 0.84 respectively. The correlation may be purely

coincidental and an artifact of the type of material. Chemical evolution from fresh to weathered could take an exponential decay trend rather than a straight line.

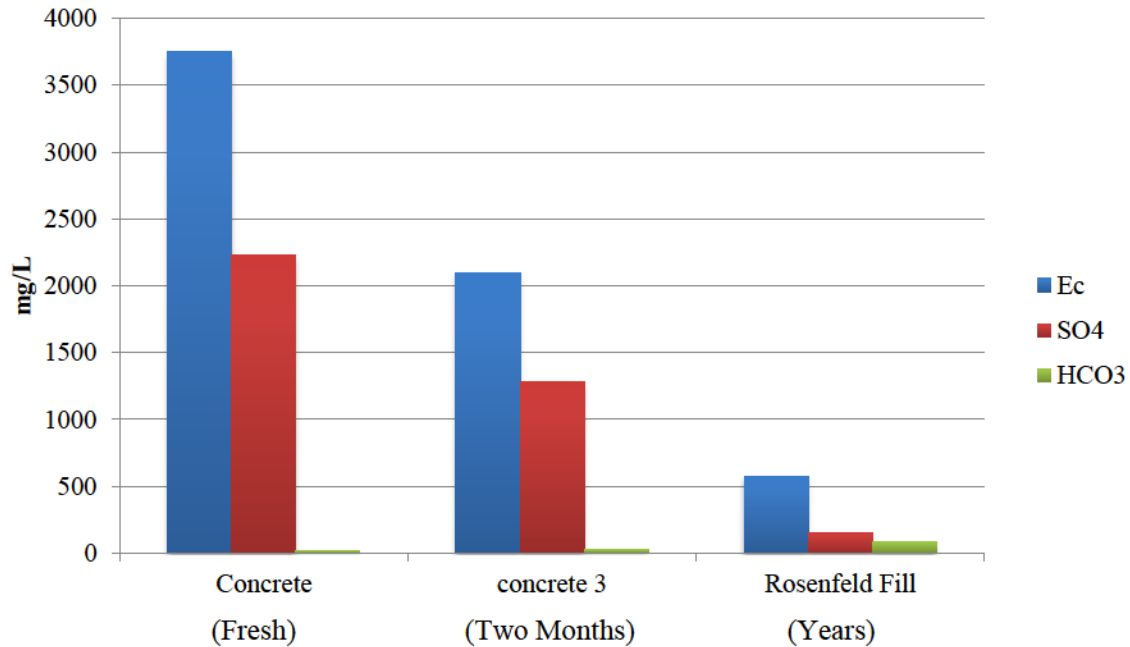


Figure 17. Comparison between fresh concrete, two months and after several years concrete (Rosenfeld anthro)

Concrete from construction debris has a high initial concentration of sulfate, which could decline quickly. The long-term weathered concrete was measured to be at concentrations within the normal range of the BRAA. Groundwater under weathered construction debris was analyzed by Urbanc (2005) and determined to be non-hazardous. The weathered state of construction seems to be essentially inert.

## *Field*

### *Resistivity*

Historic aerial photographs from 2009 show a narrow trench in figure 18a. In 2011 the photographs show a large pit that had developed, due to a mining operation, north of the trench (figure 18b). In 2012 the pit was abandoned leaving behind a pit lake (figure 18c). The filled trench, which lines the south end of the pit lake, still exists and is the focus of the resistivity study. To minimize background noise and anomalous readings a large rural field minimally affected by power grids and conductive materials, such as wire fences or metal pipes, was chosen.

Resistivity surveys were conducted on two separate days approximately 3 weeks apart. Two lines were shot during the first survey, which took place on April 25<sup>th</sup>, 2013. The survey lines were positioned to intersect areas that have been mined. The two lines trended southwest to northeast and were parallel to one another. The second survey included 3 lines perpendicular to the first set of lines shot and parallel to one another. This survey was shot on May 13<sup>th</sup>, 2013. The resistivity profiles A1 and A2 (A series) imaged the undisturbed subsurface while profiles B1, B2, and B3 (B series) imaged a portion of the filled mined pits (figure 19 and 20). Profile A1 had node 47 and 48 decouple during the electrical injection. These nodes were left out of the inversion.

The inverted resistivity values of the A and B series ranged from 1.2-127 $\Omega$  and 1.9 - 54.5 $\Omega$  respectively. The scales are independent of one another. The majority of the profiles showed three layers. The top layer was about 1.5 – 5 meters thick and had anomalous resistance changes throughout. The anomalies were irregularly shaped and consisted of mostly moderate resistivity, about 14 to 24 $\Omega$ . Borehole data showed sand in

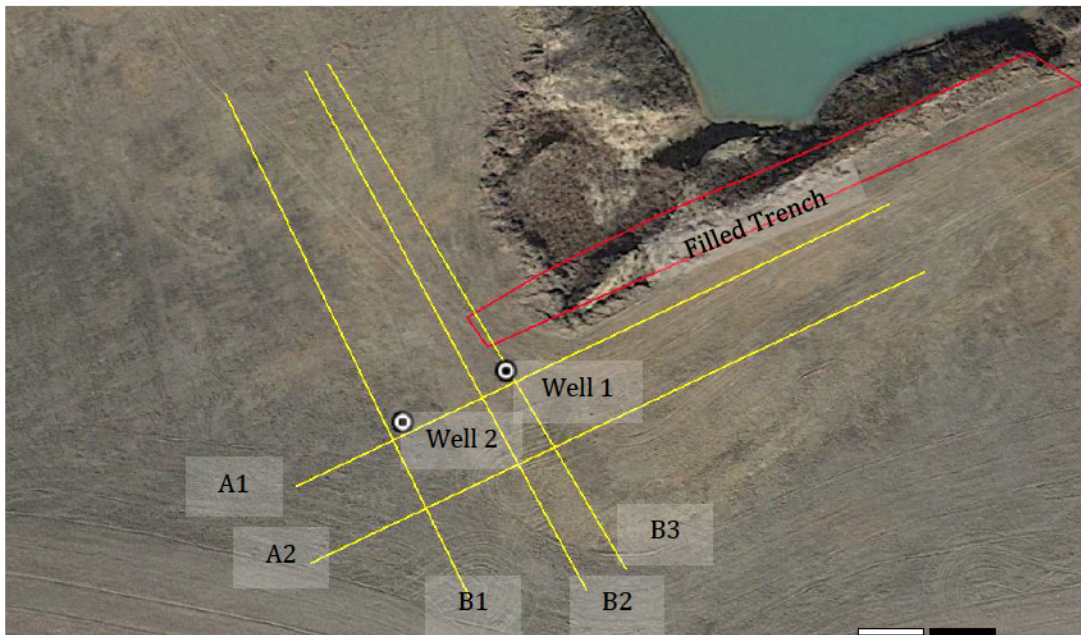
high resistivity areas and clay in the low resistance areas of the top layer (figure 20). The middle, generally more resistant layer measured from 24 to 127 $\Omega$  and was 8 – 11 meters thick. The middle layer showed more homogeneity with changes in horizontal resistivity being more gradual. Silt at middle layer depth was observed in both boreholes consistent with the homogeneity on the resistivity survey (figure 20). Below the highly resistant layer, the resistivity decreased to levels similar to the top layer for 1 to 3 meters then decreases to minimum resistant values. The third layer was the most resistant layer. This study, like Shah and others (2007), used dipole-dipole resistivity method to define a surface clay unit, the alluvium of the Brazos River alluvium aquifer, and the underlying formation. Similar patterns emerge when comparing data with the results of Shah's survey. The three-layer model was observed in both studies. The three-layer model has a conductor-resistor-conductor pattern which correlate with the hydrostratigraphic units within the area (Shah, H. Kress, and Legchenko 2007). The three-layer model agrees with the initial geologic assumption of three distinct layers: Soil/upper alluvium (conductor), lower alluvium (resistor), and shale (conductor) (figure 19 and 20). The resistivity surveys appear to be able to differentiate units within the BRAA that can be interpreted hydrogeologically. Conductive and resistant layers are associated with finer and coarser materials. Saturated thickness was estimated, from profiles along with the borehole data, to be about four meters (figure). Previous studies have estimated the BRAA to be 15-16 ft. thick (Wong 2012; J. G. Cronin and Wilson 1967)

The B series, specifically line B3, was positioned to survey the filled pit (figure). Measurements from the aerial photograph place the filled pit between 42 and 52 meters from the first node of survey B3. With an A-spacing of 2 meters, the filled pit was



a.

b.



c.

Figure 18 aerial photographs of the resistivity survey area. (a) 2009 aerial photograph of a trench in Robinson TX. The area of interest is outlined in red and super imposed onto images b and c. (b) 2011 aerial photograph of the trench now filled. North of the trench is a gravel and sand pit mining operation. (c) 2012 aerial photograph of a pit lake. Resistivity survey lines were run perpendicular and parallel to the long axis of the filled trench

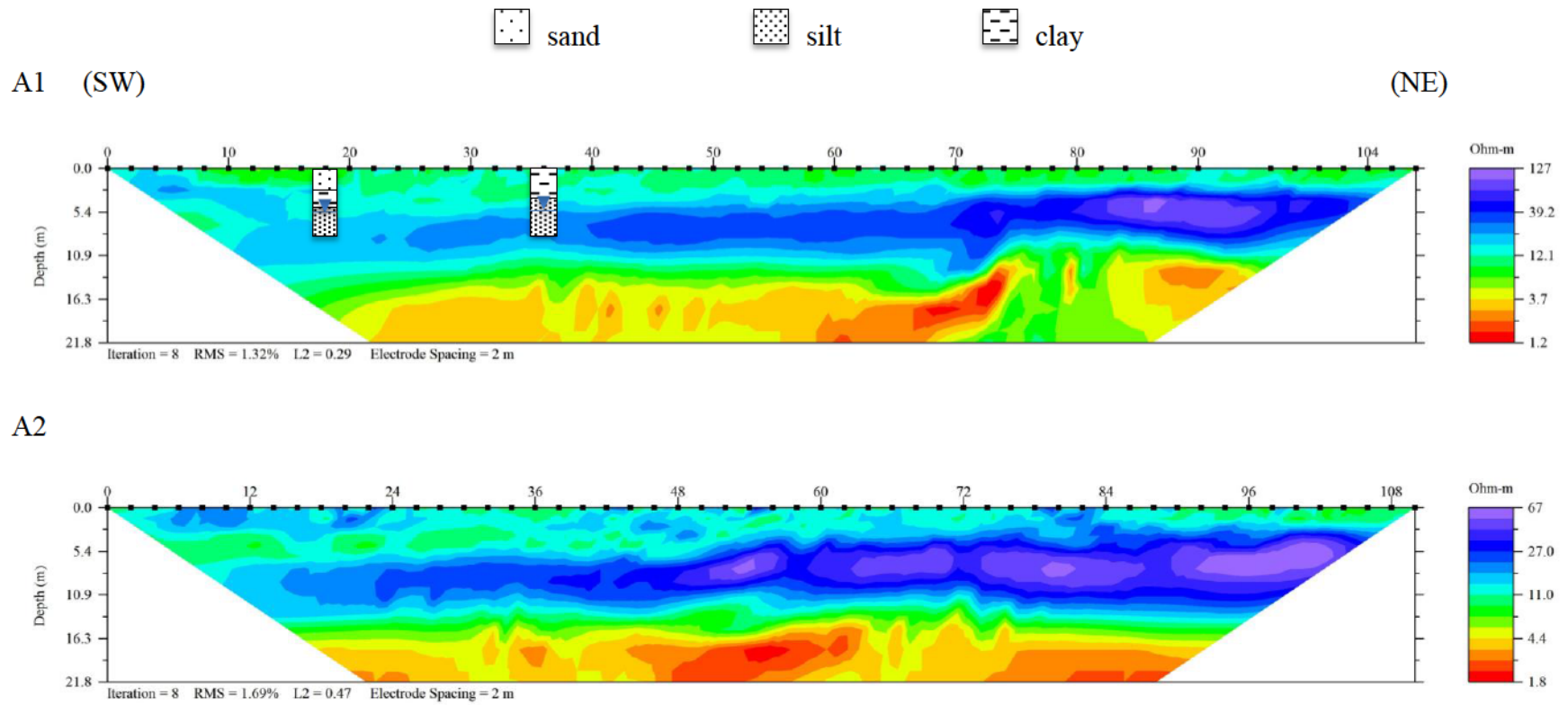


Figure 19. resistivity profiles near a filled gravel pit. The A series (A1 and A2) runs southwest to northeast and covers an area that is undisturbed.

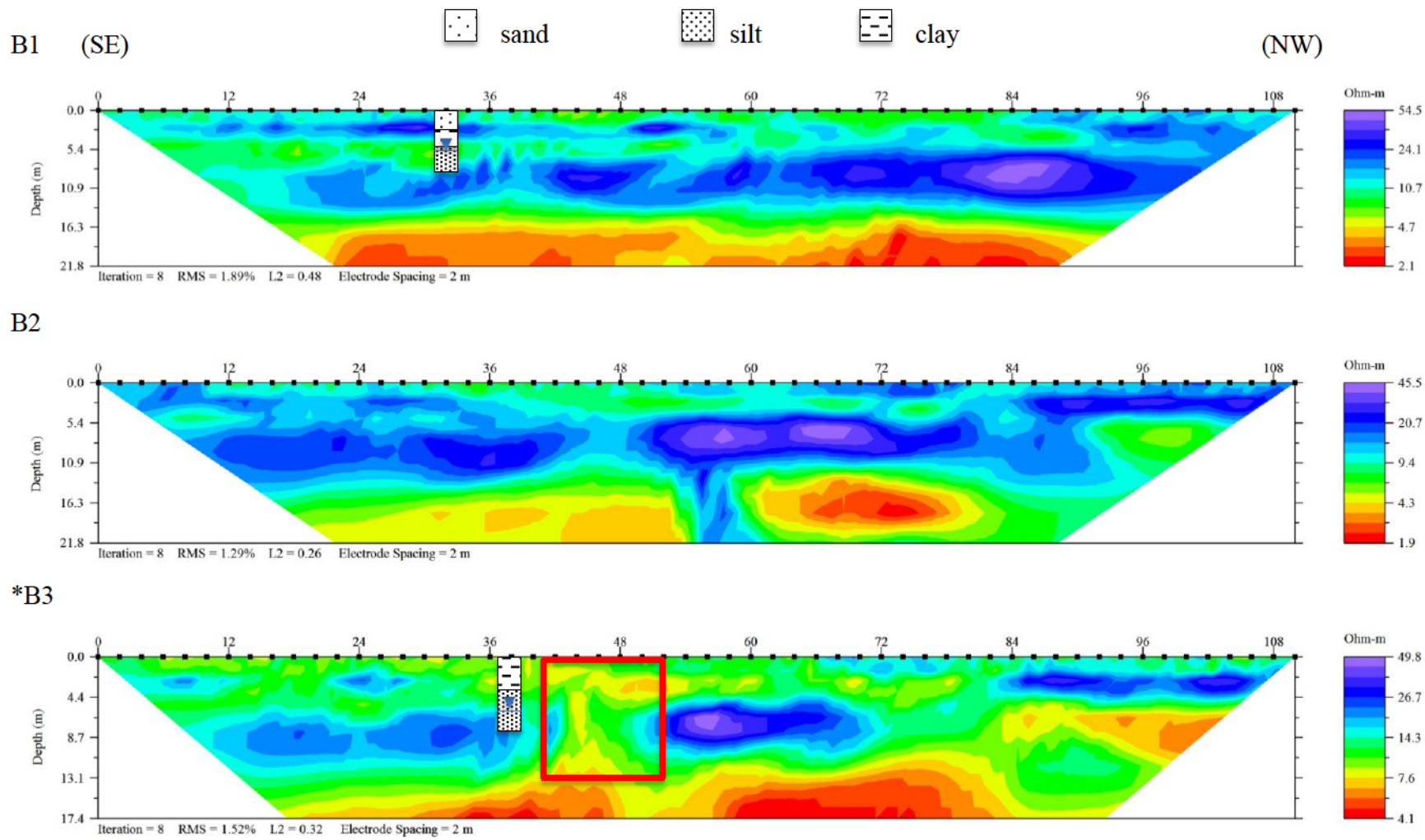


Figure 20. resistivity profiles near a filled gravel pit. The B series (B1, B2, and B3) run northwest to southeast. B1 and B2 cover an undisturbed area while B3 covers a known filled pit at nodes 21 through 26. The red box represents the filled trench crosses B3.

expected to occur between nodes 21 through 26. Profile B3 shows an anomalous low resistivity reading between nodes 21 through 26 (figure 20 B3). Resistivity readings within the expected filled area are anomalously low compared to the resistance levels of the horizontally adjacent areas on the second level. Similar readings are observed further down the line. Line B2 was placed near the edge of the filled pit and exhibited similar results to B3 but to a lesser degree. Line B1 was farther from the filled pit and more closely resembled the undisturbed pit profile.

Profile B3, from the B series resistivity survey, measured an anomaly in the same location air photos predicted infilling had occurred. A sharp boundary with resistivity differences of  $10\Omega$  exists connecting the top conductor layer with the bottom conductor layer. The anomaly had changed the normally heterogeneous resistant middle layer to a more irregularly patchy conductive layer in the filled area. The high resistance values observed in the filled area suggests finer material, most likely filled with material having similar hydrogeological characteristics as the top layer. Infilling mined areas with overburden is the most likely explanation for the resistance anomaly.

The use of 2D-DC resistivity to identify filled pits is shown to be possible but the effectiveness is not proven since the method relies heavily on field data to supplement the interpretation. Many characteristics of the site were known which enhanced the effectiveness of this particular survey. Resistivity surveying applied to an unknown area may yield results that are difficult to interpret.

## *Finite-Difference Modeling*

### *Model Setup*

The model setup for evaluating aquifer restoration in the BRAA contained an area of roughly 6,000 x 6,300 meters and consist of 35 rows and 32 columns (figure 21). The cells were not equal in dimension and range from 100 to 498m column width and 100 to 339m row width. Cell dimensions were restricted to be no larger than 1.5 times adjacent cells. The largest cells, located on the border of the grid, were non-active cells and did not interfere with calculations in the simulation.

Boundary conditions for the model were as follows:

- The eastern extent was bound by the river package (RIV), The river stage was set by interpolation between an upstream and a downstream river gauge. A free water surface (106m) was set one meter higher than the streambed surface (105m) up stream. The downstream water and streambed surface was set to 104m and 103m respectively, and interpolated in-between. Conductance of  $5.0 \times 10^{-2}$  cm/s was assigned to the river.
- No flow boundaries lined the northern and southern extent. The north and south boundaries were estimated from Cronin and Wilson (1967) water table maps.
- The western boundary of the simulated area was lined with injection wells to simulate aquifer influx. The area (A) was measured by the width (2300m) of the cells incorporating the injection wells multiplied by the saturated thickness (4m) measured from a nearby well. The gradient (I) was calculated to be  $1.3 \times 10^{-3}$  by the head difference and distance of two wells located near the west and east boundaries. The aquifer K represented the hydraulic conductivity used in the

calculation. Lateral aquifer contribution from the west boundary (Q) was calculated to be  $2.5 \times 10^{-4} \text{ cm}^3/\text{s}$  from Darcy's equation and simulated with injection wells.

The 3D finite difference model was one cell thick representing the saturated section. The saturated thickness was determined by using borehole data and the river stage where available and IDW interpolation to contour the rest. The bottoms of the cells were a no-flow boundary. The top of the model varied as the head equilibrated allowing for transmissivity to change depending on bedrock elevation and head. The hydraulic conductivity was vertically anisotropic, where  $k_x = k_y$  and  $k_z = k_x/10$ .  $K_x$  was set to  $2.0 \times 10^{-3} \text{ cm/s}$  determined by slug tests performed in the study and the permeameter tests. Recharge on the aquifer was set to four percent of mean annual precipitation (O'Rourke 2001). Four simulations were run under steady state; pre-mining, pit lakes, native filled pits, and foreign filled pits.

The first model, simulating the open pit scenario, best replicates field conditions and was used to calibrate the initial head conditions of the models. Open pit lakes were modeled with the Evaporation Package set to the mean annual evaporation rate and direct annual recharge using the Recharge Package. Permeability within the pit lake is infinite (Younger, Banwart, and Hedin 2002). The hydraulic conductivity was increased to to 100 cm/s to simulate the pit lake flow conditions. The steady state groundwater model was calibrated by comparing the contoured head data to well data collected in the fall of 2013 (appendix B). The remaining three scenarios were simulated by replacing the mined area, represented by a pink outline for figures 20 to 24, with a K representative of the fill material.

Representative K values for aquifer, native, and foreign materials were  $2.0 \times 10^{-3}$  cm/s,  $5 \times 10^{-4}$  cm/s, and 0.2 cm/s respectively derived from the permeameter and slug tests. Evaporation and direct recharge were not modeled in filled scenarios because the water table is no longer exposed.

The effects of mining and infilling mined areas to groundwater flow paths was highlighted with partial tracking using MODPATH. One particle was placed in the center of each of the twenty injection cells with particle one at the northern most well and particle twenty and the southernmost well. Particles are tracked until a boundary, designated by the program, is reached. The particles were measured for travel time ( $T_t$ ) from the injection wells to the river. Particles traveling further than the river boundary were corrected by manually checking for an arrival time at the river boundary cell.

### *Model Scenarios*

The first scenario simulated pre-mining conditions (figure 22). Head contours show a relatively smooth and slowly increasing gradient from the injection wells (119m) to the Brazos River (106m) with contour curvature increasing towards the river bend. Flow paths indicate the dominant groundwater flow direction to be perpendicular and slightly down river gradient to the Brazos River. Localized deviations flow slightly up river gradient and thought to be influenced by bedrock morphology. All particles reached the river with a  $T_t$  range of 15 – 32.6 years. Particles six and seven have the longest distance to travel and are on either side of

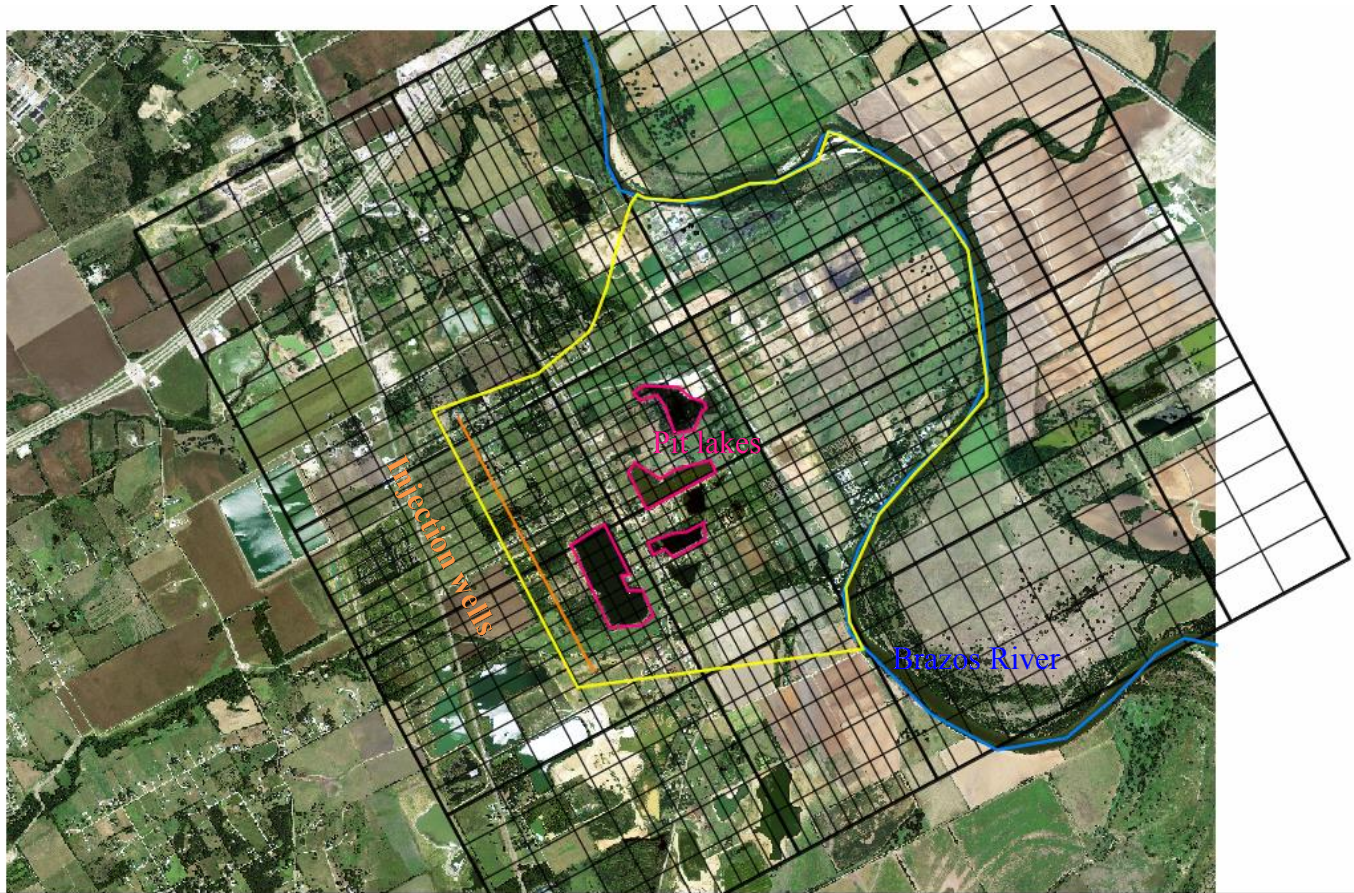


Figure 21. Finite difference groundwater grid created in MODEL MUSE. Aerial photographs Robinson TX. from the National Agriculture Imagery Program (NAIP) 2010, Boundaries include: the yellow outline includes all active cells. The blue line that traces the river is a River Package (RIV) constant head boundary. The orange line is a row of injection well (Well Package). The Pink shapes outline the sand and gravel pits used in the simulation.

the water divide (figure 22). A linear groundwater velocity ( $v_g$ ) calculation using the longest line estimated  $T_t = 30$  years. The graph in figure 22 nearly illustrates a pseudo crosssection perpendicular to the direction of groundwater flow. The graph shows an increase in  $T_t$  peaking at particle six and seven highlighting a groundwater divide. The groundwater divide is illustrated in the graph of figure 22 by a gradually more positive slope towards the divide.

The second scenario modeled the mined area as pit lakes (figure 23). Head contours show a shallow gradient to the west (116m) steepening near the river (106m). Contour lines up gradient from the pit lakes curve opposite the river meander. Groundwater flow in the pit lake region is dominated by through-flow. Down-gradient, contour lines were similar to scenario one leading to comparable flow paths. The majority of the particles ended up in the largest modeled pit lake (figure 23). Particles six to eighteen concentrate in the pit lake where they remained with a  $T_t$  range of 5 - 11.6 years. Particles five and nineteen did enter the same lake as the trapped particles but flowed out and reached the river at a  $T_t$  of 32 year and 29.5 respectively. Particle one, three, and four had  $T_t$  of 18.5 – 25. Particles three and four traveled through a smaller pit lake and reached the discharge point with a  $T_t$  of 25 and 22.7 years respectively. The particles that did not enter a pit lake (one, two and twenty) flowed to the river with a  $T_t$  of 20 – 28 years.

Three areas appear to be influencing groundwater flow paths with pit lakes. The first area deals with groundwater flow within the mined area. Lowered water levels in pit lakes have caused drawdown effects, driven by evaporation. True “through flow” lake conditions occurred in the small pit lakes often times speeding

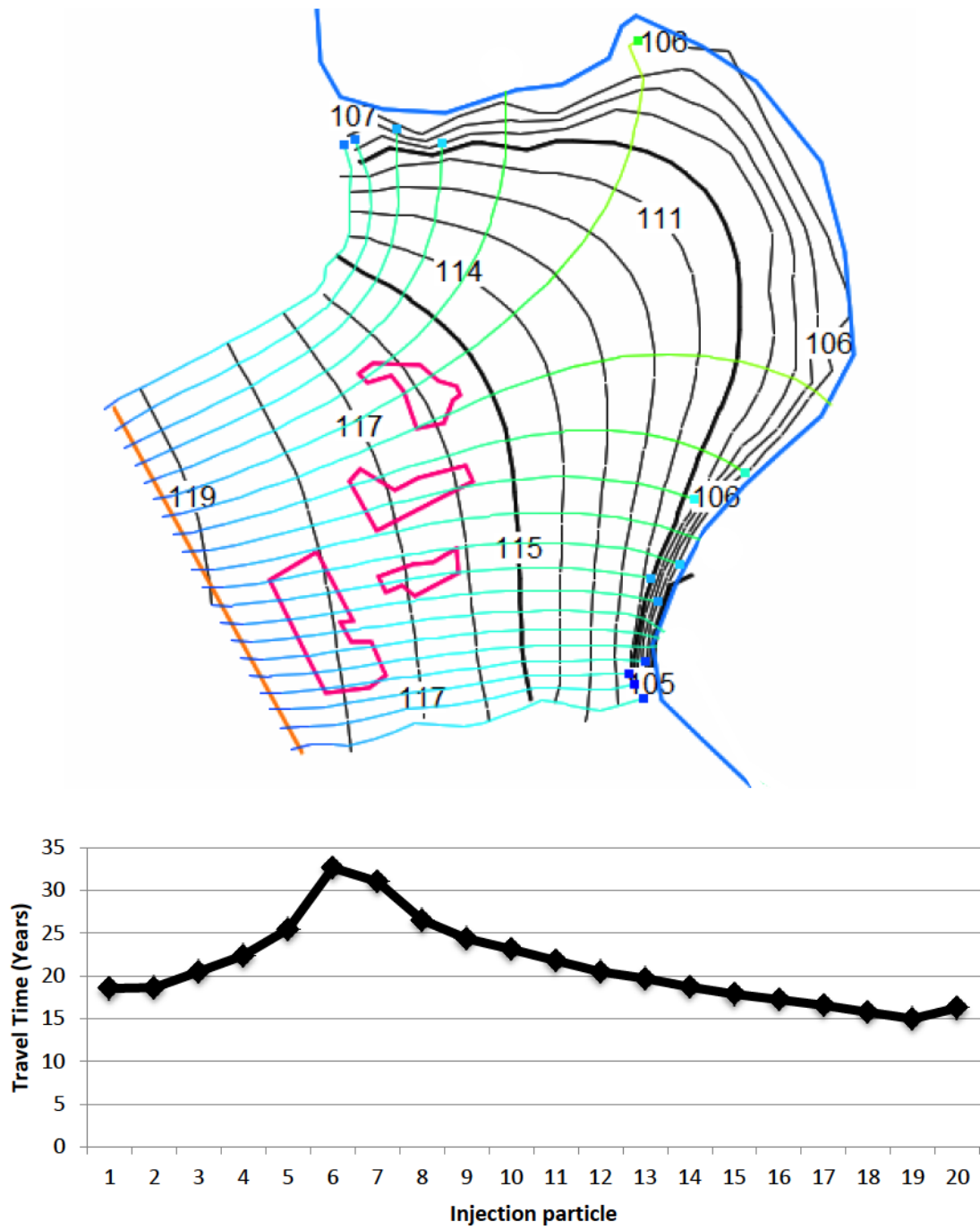


Figure 22. Head contour map of scenario one (pre-mining) with a travel time vs. particle injection cell, graph.

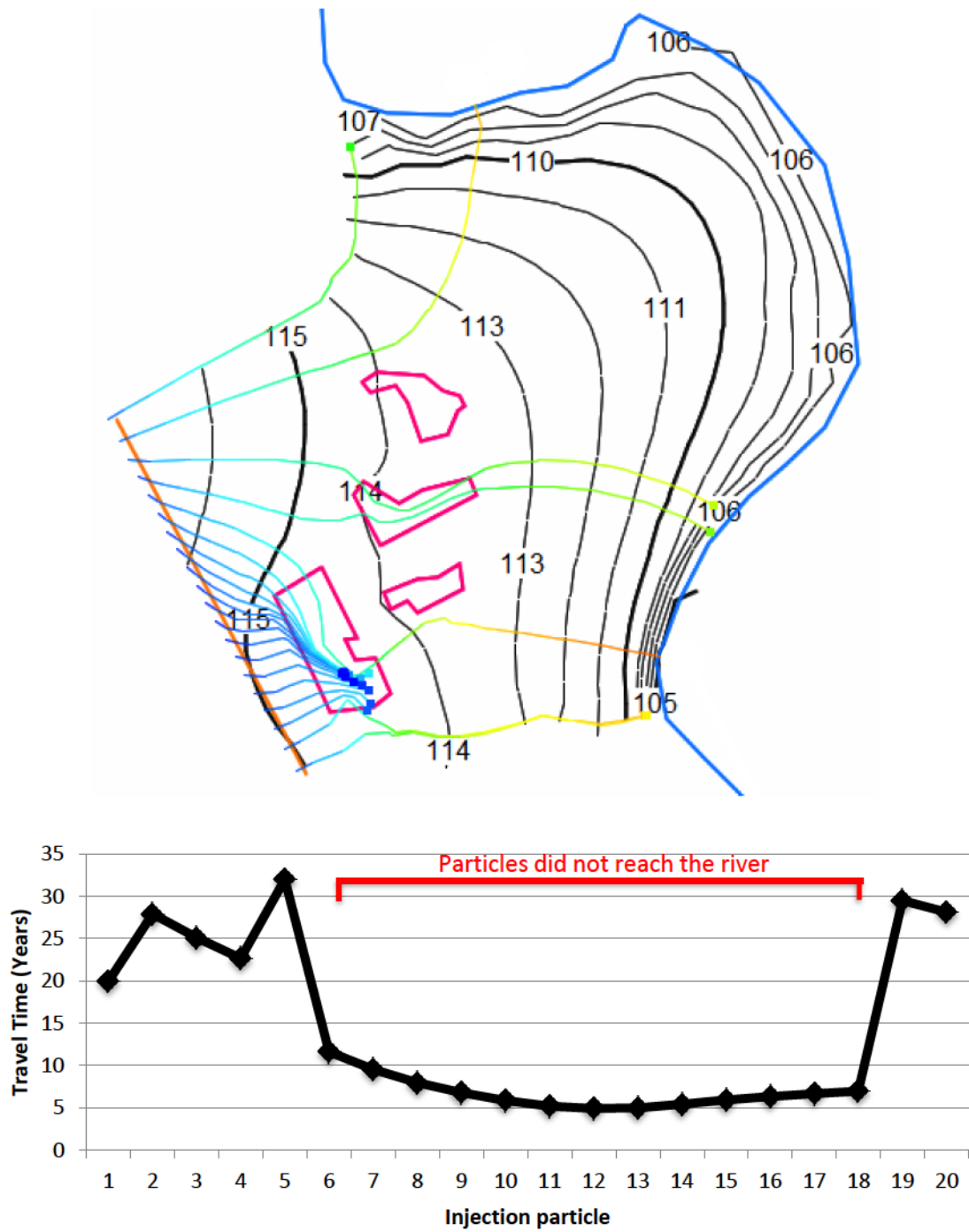


Figure 23. Head contour map of scenario two (pit lakes) with a travel time vs. particle injection cell, graph.

up particles within the lake. Particles in the larger open pit lakes were often unable to overcome the head pressure difference created by drawdown and remained in the lakes. Particles five and nineteen overcame the pressure difference and exhibited “through flow” lake conditions. A 3-D view of particle five showed vertical movement up to the water table before returning to the deeper water extending residence time in the lake and increasing  $T_t$ . With drawdown occurring inside the pit lake system, the aquifer surrounding the lake discharged into the lowered head surface affecting an area around the lake or the area of influence (AOI). The second mechanism influenced the groundwater flow outside of the mined area observed from the particles response to preferentially move towards pit lakes. Deviated flow paths often increased the distance traveled and therefore  $T_t$  of a particle. Flow paths that did not deviate towards the pit lakes were interpreted to be outside of the area of influence (AOI). These particles were affected instead by the aquifer’s response to the groundwater gradient reduction from pit lake draw down (the third mechanism). Gradient reduction leads to slower  $T_t$  outside the AOI.

The third scenario modeled mined areas filled with native material (figure 24). Head contours range from 119m to 106m. Contours near the mined area are semi-irregular but maintain a generally convex shape following the river bend. Contour curvature increases toward the river, down gradient. Flow paths approaching the up gradient side of the filled pit preferentially move to the sides and seldom into the filled area. The flow paths converge slightly on the down gradient side but not completely. The first six particles have little to no deviation and have a  $T_t$  of 17 – 23 years. Flow path deviation decreased from particles fifteen to twenty

with  $T_t$  ranging from 12 - 22 years. Particles seven through fourteen had a mixture of flow paths that pass through filled pit areas, with  $T_t$  ranging 24 – 32 years, or weave in between them,  $T_t$  ranging 19 – 24 years.

Groundwater retardation within native material filled pits had nominal impact on  $T_t$  for a small number of particles identifiable by the two high points represented in the graph of figure 24. Between the two peaks the  $T_t$  dropped slightly below pre-mining  $T_t$ . These were the particles that maneuvered between filled areas. The tendency for particles to preferentially flow around the filled area suggests AOI and the aquifer response to native material to be a bigger factor in changing aquifer function. The AOI keeps groundwater flow in the more hydraulically conductive pathways decreasing the  $T_t$  of the majority of the particles. The  $v_g$  was also increased by less permeable native material damming the groundwater and increasing head on the up dip side of the pits. The change in gradient decreased the  $T_t$  of the particles outside of the AOI to less than the pre-mining conditions.

The fourth scenario modeled the mined area filled with foreign type material (figure 25). Head contours show a shallow gradient to the west (118m) steepening near the river (106m). Particles in a swath slightly larger than the filled areas preferentially flow towards the filled area from the up dip side. Flow paths are bottlenecked in the filled area then fan out as they exit on the down dip side, opposite the manner they entered (figure 25). Flow paths further up and down gradient appear less altered (figure 24). Particles observed to have moved through multiple filled areas generally had the lowest  $T_t$  ranging 13 – 20 years. The particles moving through one pit had a  $T_t$  of 14 – 28 years. The flow paths not cutting through

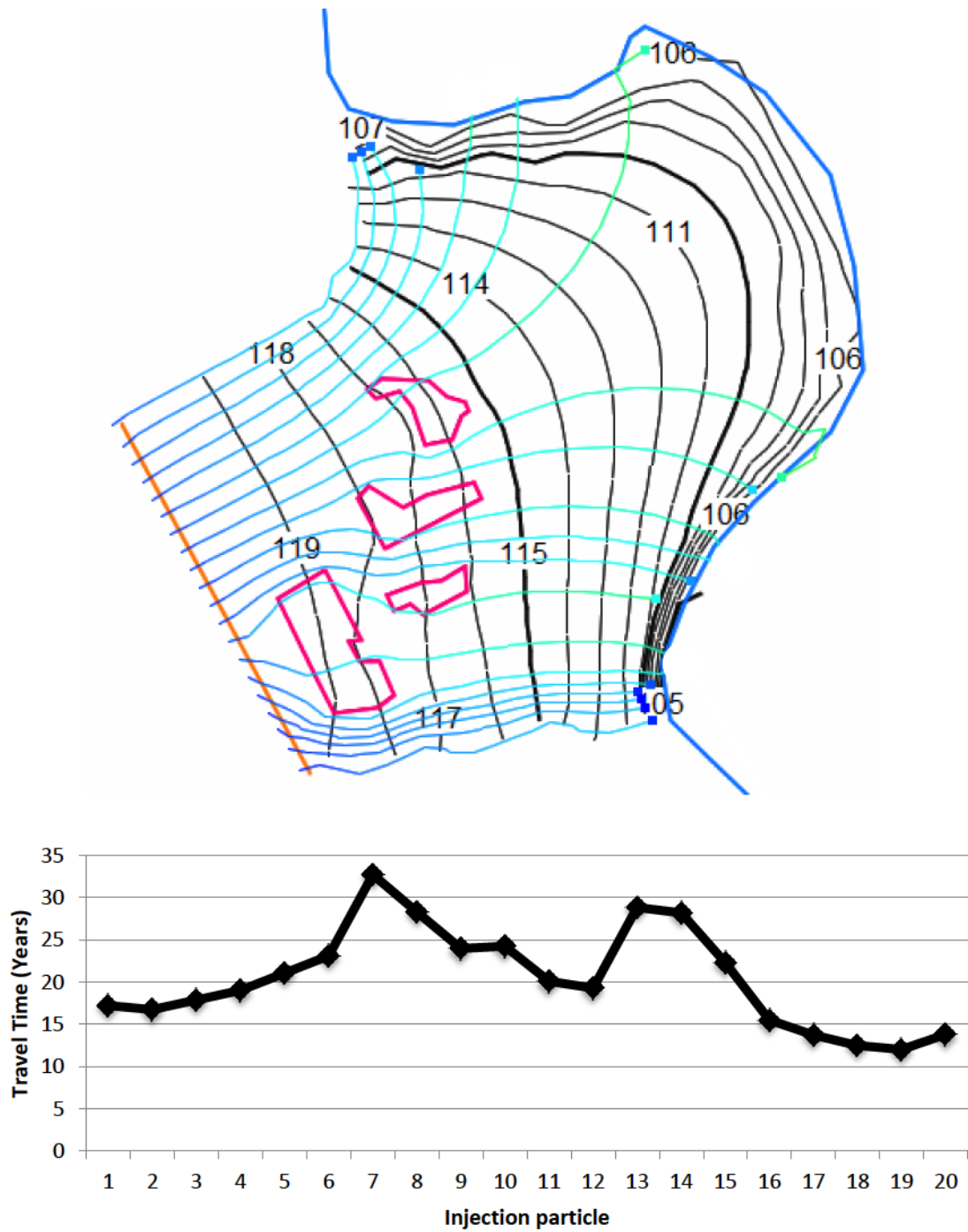


Figure 24. Head contour map of scenario three (native fill) with a travel time vs. particle injection cell, graph.

filled areas registered a  $T_t$  of 21 – 25 years. Particle five took the longest flow path estimated at 35 years.

The foreign material affected the aquifer by reducing the overall water table. The reduction in head pressure created low flow velocity conditions outside of the filled area. Figure 25 shows three peaks representing particles that traveled outside of the AOI or had longer travel distances. The reduced  $v_g$  increased particle  $T_t$  with in the overall aquifer. Particles with decreased  $T_t$  was attributed to increased flow rates in filled areas caused by the material's higher permeability. Decreased  $T_t$  was found to have a relation to the ratio of flow path distance inside and outside of filled areas. Flow paths cutting through multiple filled areas illustrated this relationship with even lower particle  $T_t$  (figure 25). The filled area was observed to have a narrow AOI. Flow paths between filled areas tended to bend towards filled areas increasing path distance and residence time in the aquifer.

The particle  $T_t$  plots were combined to compare the pre-mining flow condition to all other scenarios modeled (figure 26). The interior injection cells, from cell six to eighteen, highlight groundwater flow inside mined areas and within the AOI. The cells at the flanks better represent the aquifer response to these mining activities. The boundary between the interior and flanks vary with each scenario but generally start where the lines initially cross the pre-mining line and ends with the lines re-crossing the pre-mining line at the opposite end. The interior width may have some relation to the AOI.

The interior injection particles for the pit lake scenario inhibited the particles from reaching the river by concentrating most of the particles in the lakes and cannot be compared to the other results. A concern that arises from evaporative concentration in pit

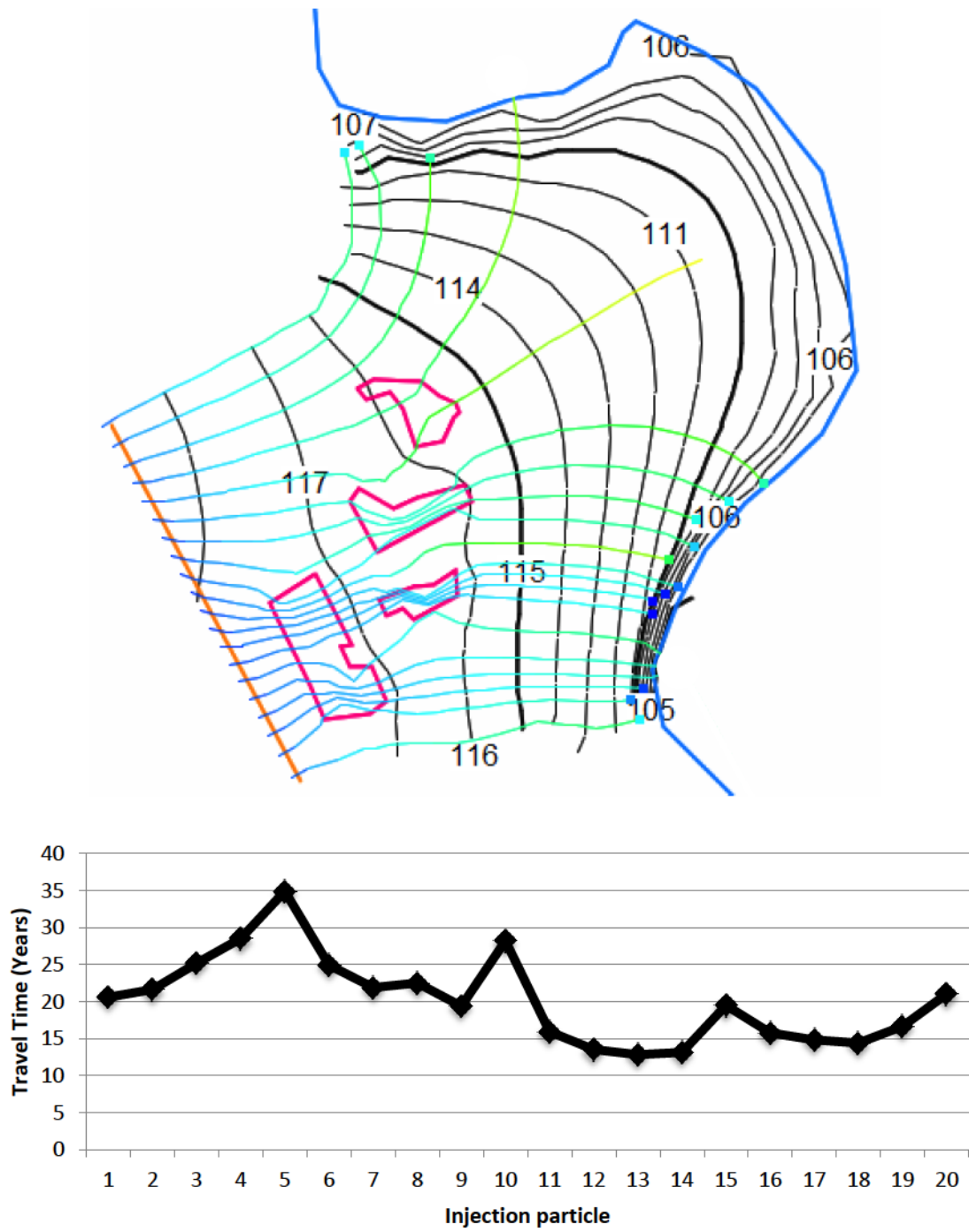


Figure 25. Head contour map of scenario four (foreign fill) with a travel time vs. particle injection cell, graph.

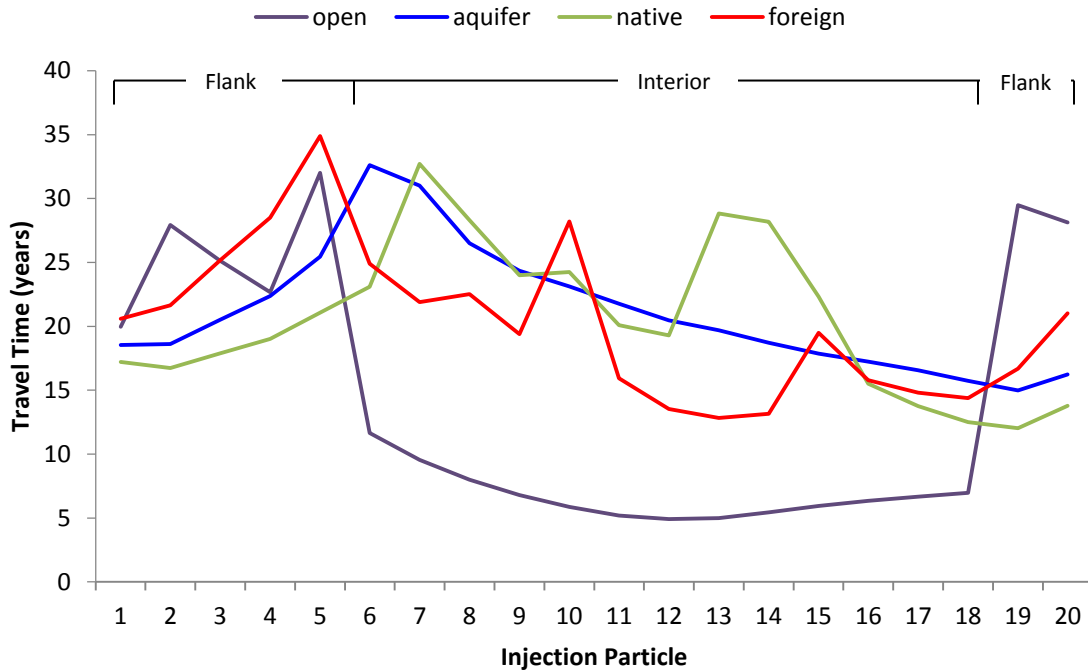


Figure 26. Composite of travel time graphs for all four scenarios.

lakes, already susceptible to direct contamination, is concentrated pollution. In the dry season, evaporation will exceed the modeled potential and in the wet season the recharge flux may mobilize the concentrated pollutants. Theoretically, the pit lakes are a zone of infinite permeability and could speed up the contaminant flux discharge into the river after high recharge events. The contamination issue is lessened with material filling in mined pits

Foreign materials and native materials used to fill pit lake areas create flow regimes more similar to pre-mined conditions. The difference between the fill materials is rooted in their permeability. Morgan-Jones and others (1984) had described groundwater flow in less-permeable native fill as an impedance of groundwater causing diverged flow lines upstream of the infill. In contrast, foreign fills have higher permeability concentrating up stream flow into the mined areas decreasing  $T_t$ . Figure 26

shows native fill and foreign fill interior particle travel times as generally inverse from one another.

Both fill materials offer a buffer to surface sourced contamination but have differences in the mobilization of constituents in the saturated zone. Low-K native fill slows the movement of groundwater in what may have been a high production gravel lens. High-K foreign fill increased the movement of groundwater higher than pre-mining conditions. The permeability used for pre-mining conditions was measured in finer material and not in the high production zones. The discrepancy between foreign fill and aquifer sand and gravel permeability, measured in the permeameter, is much less and may be a better representation of the actual material replacement.

The flow dynamics in the flanks responded to head changes in the aquifer. Larger differences in head increase  $v_g$  on the flanks. High permeability materials allow for quicker discharge into the river dropping the head elevation. Production in the flanks would drop with high-k fill but overall production would be enhanced.

The finite-difference model with particle tracking has illustrated that pit lake conditions are vastly dissimilar to the pre-mining conditions and that both fill material would be an improvement in reestablishing an aquifer flow regime.

## CHAPTER FOUR

### Summary and Conclusions

Gravel mining area in the Brazos River floodplain continually expands with effects to aquifer budget and flow regime in the BRAA. Although the sample size and special representation of samples could be improved, this study estimates the current state of mining on the BRAA and provides suggestions to create a sustainable aquifer framework for the future production demands.

1. Spatial data suggest open pit lakes, an ever-increasing fraction of the aquifer, are a large influence in decreasing the water budget due to evaporation. A budget analysis estimated the ratio of evaporation to direct recharge to be 1.7.

2. Hydrogeologically native fill materials are the least hydraulically conductive followed by the aquifer material. Aquifer materials tested in the laboratory measured higher than slug tests performed in the field. The scale of the two tests and selectiveness of the lab test samples contributed to the discrepancy in K. Foreign materials were the most hydraulically conductive but showed a large range, likely due to the large particle size and poor sorting of anthropogenic materials.

3. Chemically native and aquifer-derived waters are ionically similar. Foreign material water chemistry was influence by foreign materials. Construction debris was the most common anthropogenic material found in foreign fill, which elevated sulfate concentrations. Leaching experiments showed fresh concrete sulfate concentrations to decrease over time. Weathered construction material ion concentrations were within the measured concentration ranges observed naturally in the BRAA.

4. Two-dimensional direct-current resistivity with dipole-dipole array was successfully used to differentiate horizontally continuous fine-grained and coarse-grained layers in the Brazos River alluvium. Fine-grained fill material was imaged as a vertical structure truncating the coarse layer containing the BRAA. Resistivity methods are capable of identifying fill materials in shallow alluvial aquifers.

5. MODFLOW 2005 with MODPATH was used to understand the flow dynamics of the BRAA in response to infilling mined areas. Results suggest both native and foreign materials would reduce groundwater flow influenced by evaporative loss. Low-permeability native material acts as a barrier to groundwater flow. High-K foreign material increases groundwater flow velocity but decreases the overall water table elevation.

6. Foreign material has the greatest potential for filling mined areas in terms of production. Native materials have an average permeability less than the aquifer material, which is not desirable in restoring aquifers production but could be used to decrease evaporation. Some foreign materials, like construction debris and chalk, have a K similar to the highly productive sand and gravels. Filling gravel pits with chemically inert, high-k foreign material could restore the aquifer framework and production potential of the BRAA combined with native overburden could restore land topography. Native overburden fill, original to the site, could be placed on top of the foreign material to restore the fining upward sediment distribution and act as the natural buffer to contaminants.

## CHAPTER FIVE

### Recommendations

1. Aquifer Framework Restoration should be intentional and purpose to restore general aquifer characteristics.
2. Coarse, permeable fill, whether anthropogenic or natural should be placed in the bottom of the pit and covered with finer grained material up to the surface. This mimics the natural fining upward sequence protecting the groundwater from direct evaporation and contamination from above while resulting in a productive water table aquifer.
3. Fill should be composed of materials that do not contaminate the groundwater.
4. More testing on the water quality effects of construction waste material such as broken bricks, concrete, and excavated rock rubble should be conducted before they are used.

## APPENDICES

## APPENDIX A

### Porosity Measurements for Fine-grained Samples

Table A1. Porosity calculation for fine-grained material

a. Bulk samples

sample	cylinder	Total mass (container + sediment + tin) (g)	dry weight (C+S+T)	dry weight (s)	Bulk Density (Db)	wet weight (s)	water weight (g)	water volume (cm <sup>3</sup> )	solid volume	Dp	% porosity
Equestrian	A	720.8	604.5	535.85	1.60	652.15	116.3	116.3	219.22	2.44	34.66
new pit	B	667	527.4	459.76	1.43	599.36	139.6	139.6	182.74	2.52	43.31
lockwood native	C	788.2	653.2	586.06	1.77	721.06	135	135	196.16	2.99	40.77
austin	A	755.3	624.2	555.55	1.66	686.65	131.1	131.1	204.42	2.72	39.07
rosenfeld native	B	629.7	493.8	426.16	1.32	562.06	135.9	135.9	186.44	2.29	42.16
for sale	C	694.1	569.3	502.16	1.52	626.96	124.8	124.8	206.36	2.43	37.69
tan pile	B	700.2	569.7	502.06	1.56	632.56	130.5	130.5	205.02	2.45	36.40
locked gate	C	693.4	552.4	485.26	1.47	626.26	141	141	181.34	2.68	45.24

b. Sample instrument mass and dimensions.

shelby tube container	diameter (cm)	average mass of container (g)	Cylinder Volume (cm <sup>3</sup> )	Tin (g)	tin + container (g)
A	7.60	60.49	335.52	8.1	68.65
B	7.55	59.54	322.34	8.1	67.64
C	7.60	59.04	331.16	8.1	67.14

## APPENDIX B

### Well Data

Well No. Ju-1 Date: Mar. 30, 2013 Time: 10:05 am

Bore hole water measurements: Well casing: 10 ft screen at the bottom and 11.2 ft. pvc for a total of 21.2 ft. cased well

Water depth @ 17.2 ft. Below the surface

Depth to bedrock = 27 ft. Below the surface

T=21.8 C

Ec=759 mms

Other Comments: The casing was pressed into the borehole from a depth of 19 ft. to 21.2 ft. The borehole collapsed up to 19 feet depth with in two hours of drilling. Development of the borehole was accomplished using a bailer.

Well Development : April 2, 2013

Water depth @ 17.1 ft.

T=21.7 C

Ec= 770mms

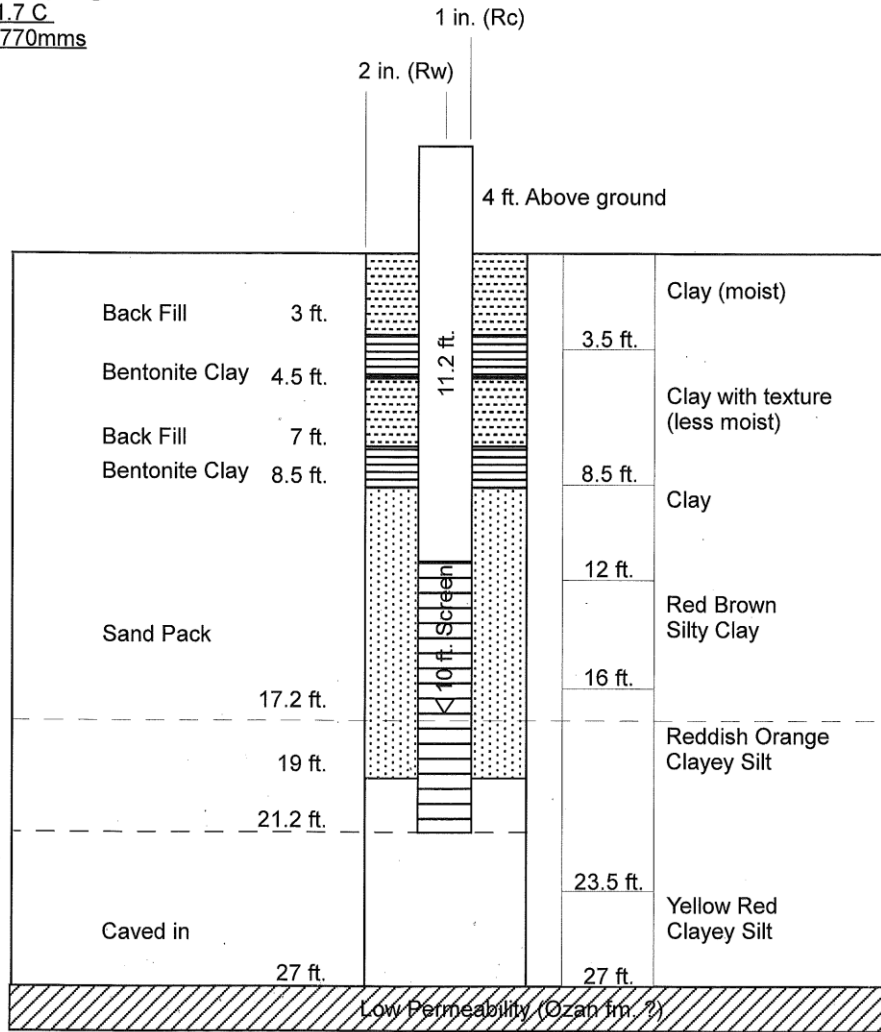


Figure B1. Well-1 used to field check resistivity survey

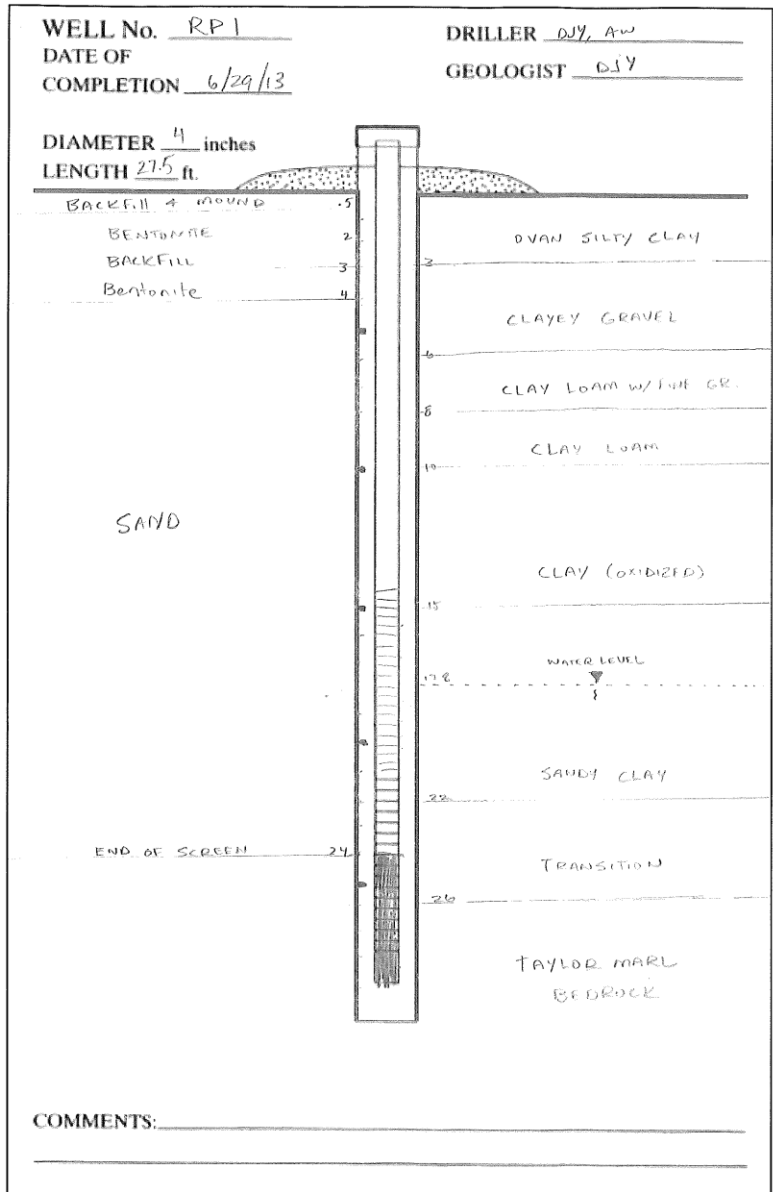
WELL No. <u>RPI</u>	DRILLER <u>Dr. Joe Yelderman</u> <u>Andrew Worcester</u>
DATE OF COMPLETION <u>6/29/2013</u>	GEOLOGIST <u>Dr. Joe Yelderman</u>
DIAMETER <u>4</u> inches	N <u>31° 29.583'</u>
LENGTH <u>27.5</u> ft.	W <u>97° 05.394'</u>

<p>CASING <u>20'</u></p> <p><u>2</u> inch</p> <p>Material <u>PVC</u></p> <p>Depth <u>14</u> ft</p>	<p>SURFACE SEAL</p> <p>Type <u>Bentonite</u></p>
	<p>HOLE DIAMETER</p> <p><u>4</u> inches</p>
	<p>ANNULAR SEAL</p> <p>Type <u>backfill</u></p> <p>Depth <u>2 - 4</u> ft</p>
	<p>Bridging?</p>
<p>SCREEN <u>10'</u></p> <p><u>2</u> inch</p> <p>Material <u>PVC Slotted</u></p> <p>Depth <u>14 - 24</u> ft</p>	<p>FILTER PACK</p> <p>Type <u>SAND</u></p> <p>Depth <u>4 - 24</u> ft</p>
<p>STATIC WATER LEVEL</p> <p><u>23.33</u> ft below TOC</p> <p><u>7/3/13</u></p> <p>Date</p>	<p>DEPTH</p> <p>TD <u>27.5</u> ft</p> <p>Plugged-back <u>2.5</u> ft</p>

COMMENTS: \_\_\_\_\_

Figure B2. Well-2 used to field check resistivity survey. a. well completions.



- Take off screen in Template  
 - extend hole in diagram

b. Well-2 lithological description.

Table B1. Well completion data for two wells on the Hirsh Dairy with slug-test data.

**HD1:**

total depth: 34'  
 screen length: 30'  
 TOC: 5.6'  
 PVC width: 2"

Slug-test result. 0.0009 cm/s,

**HD2:**

total depth: 29'  
 screen length: 25'  
 TOC: 5.83'  
 PVC width: 2"

Slug-test result. .0007 cm/s.

Table B2. Model calibration wells.

Well	Depth to water table (ft Below surface) (11/14/13)	Elevation of water table (m)	Model location (col, row)	Model water table
HD 1	34.73	106.73	28,9	107.64
HD2	30.34	110	23,9	111.2
HD3	27.37	107.462	24,10	110.9

Table B3. Estimated particle travel times (in hours) from injection well to river.

	open	aquifer	native	foreign
1	19.9	18.5	17.2	20.5
2	27.9	18.6	16.7	21.6
3	25.1	20.5	17.8	25.1
4	22.6	22.3	19.0	28.5
5	32.0	25.4	21.0	34.9
6	11.6*	32.6	23.0	24.9
7	9.5*	31.0	32.7	21.9
8	7.9*	26.5	28.3	22.5
9	6.7*	24.3	23.9	19.3
10	5.8*	23.1	24.2	28.2
11	5.1*	21.7	20.0	15.9
12	4.9*	20.4	19.2	13.5
13	4.9*	19.6	28.8	12.8
14	5.4*	18.7	28.1	13.1
15	5.9*	17.8	22.3	19.4
16	6.3*	17.2	15.5	15.7
17	6.6*	16.5	13.7	14.8
18	6.9*	15.7	12.4	14.3
19	29.4	14.9	12.0	16.6
20	28.1	16.2	13.7	21.0

\*Particles that did not reach the river

## APPENDIX C

### Chemical Data

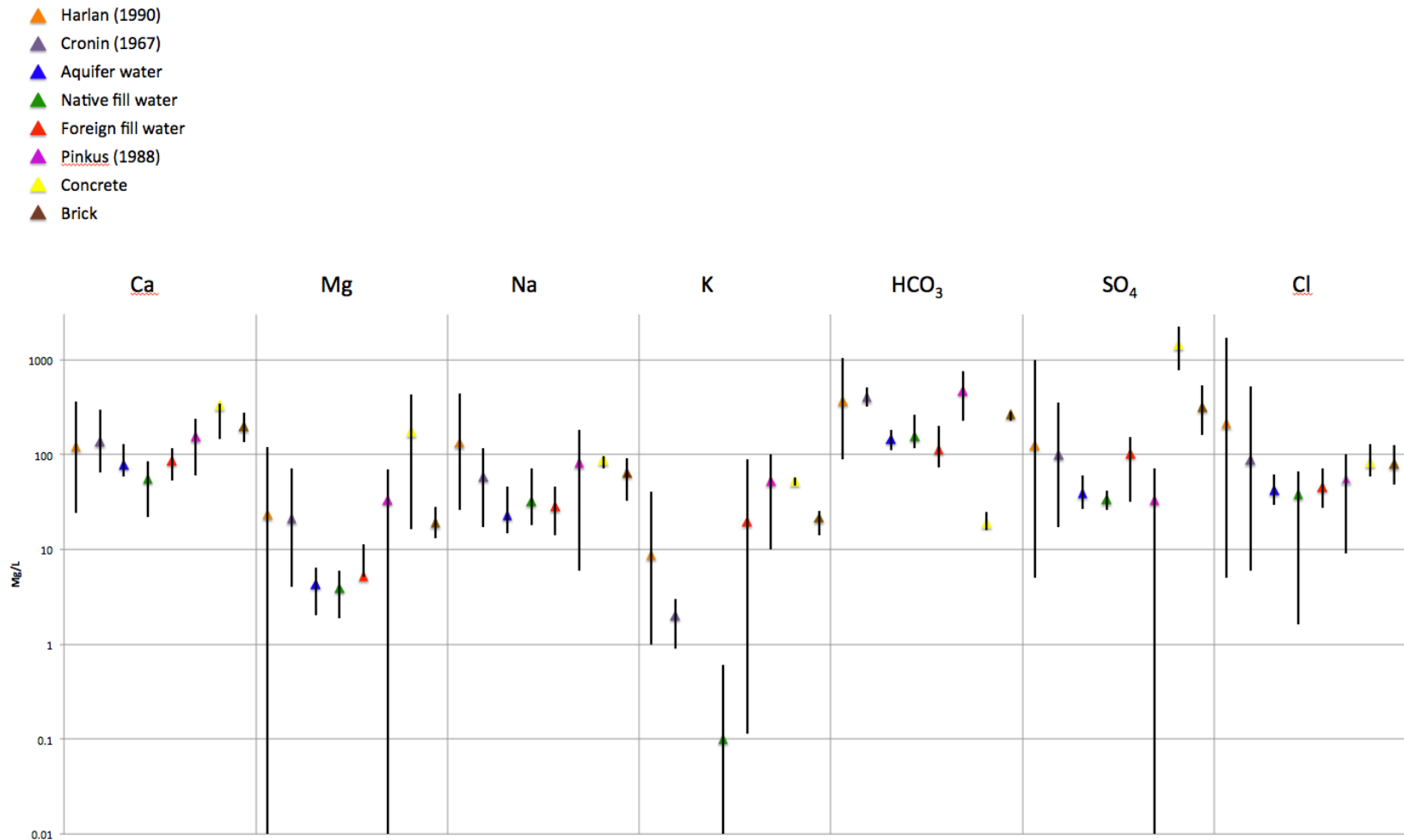


Figure C1. Comparison of analyzed water data to field investigations conducted by Cronin (1967), Harlan (1990), and Pinkus (1987). The maximum, minimum, and mean (the triangle symbol) are provided for calcium, magnesium, sodium, potassium, bicarbonate, sulfate, and chloride.

Table C1. Min, mean, and max ion concentrations (mg/L) by material type.

Type	Cl	SO <sup>4</sup>	N	F	PO <sup>4</sup>	K	Ca	Na	Mg	HCO <sup>3</sup>
Aquifer										
max	61.61	59.56	29.86	0	0	0	127	45.89	6.39	181.15
mean	41.79	38.85	19.91	0	0	0	77.8	22.8	4.28	145.1664
min	29.12	26.4	0	0	0	0	58.51	14.87	2.03	110.16
Native										
max	66.82	41.55	40.68	0	0	0.59	84.52	71.34	5.98	261.94
mean	37.898	33.4	9.07	0	0	0.0988	55.38	30.9	3.911	155.244
min	1.62	25.98	0	0	0	0	21.9	18.01	1.86	117.504
Foreign										
max	70.81	153.9	114	0	0	88.48	115.1	45.89	11.42	201.96
mean	45.01	101.68	31.38	0	0	19.51	85.81	28.15	5.19	112.85
min	27.92	31.35	0	0	0	0.114	53.15	14.16	0	73.44

## REFERENCES CITED

- 92nd United States Congress. 1972. *Federal Water Pollution Control Act Amendments of 1972*. 86 Stat. 816.
- Ashworth, J.B., and Janie Hopkins. 1995. "Aquifers of Texas". 345. Texas Water Development Board: TWDB.
- Barbudo, Auxi, Adela P. Galvín, Francisco Agrela, Jesús Ayuso, and Jose Ramón Jiménez. 2012. "Correlation Analysis between Sulphate Content and Leaching of Sulphates in Recycled Aggregates from Construction and Demolition Wastes." *Waste Management* 32 (6): 1229–35.
- Bouwer, H., and R.C. Rice. 1976. "A Slug Test for Determining Hydraulic Conductivity of Unconfined Aquifers with Completely or Partially Penetrating Wells." *Water Resources Research*, no. 12: 423–28.
- Buttleman, Cynthia G. 1992. "A Handbook for Reclaiming Sand and Gravel Pits in Minnesota". St. Paul, Minnesota: Department of Natural Resources.
- Canter, L.W. 1982. "Overview of Aquifer Restoration." *Proceeding of the Second National Symposium on Aquifer Restoration and Ground Water Monitoring*, 4.
- Castro, J. M., and J. N. Moore. 2000. "Pit Lakes: Their Characteristics and the Potential for Their Remediation." *Environmental Geology* 39 (11): 1254–60.
- Cronin, James G., and Clyde A. Wilson. 1967. "Ground Water in the Flood-Plain Alluvium of the Brazos River, Whitney Dam to Vicinity of Richmond, Texas". 41. Austin, Texas 78711: U.S. Geological Survey.
- Crystal, R.M., and R.W. Heeley. 1983. "Comprehensive Aquifer Evaluation and Land-Use Planning for Aquifer Restoration and Protection in Action, Massachusetts." *Proceeding of the Third National Symposium on Aquifer Restoration and Ground-Water Monitoring*, 175–85.
- Dibonito, M, N Breward, N Crout, B Smith, and S Young. 2008. "Overview of Selected Soil Pore Water Extraction Methods for the Determination of Potentially Toxic Elements in Contaminated Soils Operational and Technical Aspects." In *Environmental Geochemistry*, 213–49. Elsevier. <http://nora.nerc.ac.uk/3943/>.
- Epps, L.W. 1973. "A Geologic History of the Brazos River." *Baylor Geological Studies Bull*, no. 24: 44.

- Erwin, K. 1991. "An Evaluation of the Wetland Mitigation in the South Florida Water Management District, Vol. 1." Report to the South Florida Water Management District. West Palm Beach, Florida, U.S.A.
- Finger, S.E., S.E. Church, and P. von Guerard. 2007. "Potential for Successful Ecological Remediation, Restoration, and Monitoring." *U.S. Geological Survey Professional Paper 1651*, 1,096.
- Glasser, Fredrik P., Jacques Marchand, and Eric Samson. 2008. "Durability of Concrete — Degradation Phenomena Involving Detrimental Chemical Reactions." *Cement and Concrete Research* 38 (2): 226–46.
- Graf, William L. 2001. "Damage Control: Restoring the Physical Integrity of America's Rivers." *Annals of the Association of American Geographers* 91 (1): 1–27.
- Grandy, Catherine J., Paul L. Younger, John Henstock, Toby Gill, and Duncan Wardrop. 2004. "The Hydrogeological Behaviour of Flooded Sand and Gravel Pits and Its Implication for Functioning of the Enclosing Aquifer". Upon Tyne, UK: University of Newcastle.
- Harbaugh, A.W. 2005. "MODFLOW-2005, The U.S. Geological Survey Modular Ground-Water Model—the Ground-Water Flow Process: U.S. Geological Survey Techniques and Methods 6-A16."
- Harlan, S.K. 1990. "Hydrogeologic Assessment of the Brazos River Alluvium Aquifer Waco to Marlin, Texas". Unpub. master's thesis, Waco, TX.: Baylor University.
- Harlan, S.K. 1985. "Hydrogeologic Assessment of the Brazos River Alluvial Aquifer Waco to Marlin, Texas". Unpub. Bachelor's thesis, Waco, TX.: Baylor University.
- Hatva, T. 1994. "Effects of Gravel Extraction on Groundwater." *Future Groundwater Resources at Risk Proceedings of Helsinki Conference* 222. IAHS Pub: 427–34.
- Hibbs, B. J., and J. M. Sharp. 2012. "Hydrogeological Impacts of Urbanization." *Environmental & Engineering Geoscience* 18 (1): 3–24.
- Hill, R.T. 1901. "Geology and Geography of the Black and Grand Praries". United States Geological Survey Twenty-First Annual Report.
- Hobbs, S.L., and J. Gunn. 1998. "The Hydrogeological Effect of Quarrying Karstified Limestone: Options for Prediction and Mitigation." *Quarterly Journal of Engineering Geology*, no. 31: 147–57.
- Loke, M.H. 2004. "Tutorial: 2-D and 3-D Electrical Imaging Surveys". Houston, TX.: Geotomo.

- M.G., McDonald, and A.W. Harbaugh. 1988. "A Modular Three-Dimensional Finite-Difference Ground-Water Flow Model." In *U.S. Geological Survey Techniques of Water-Resources Investigations, Book 6*.
- Maguire, C.E. 1985. "Wetland Replacement Evaluation". DACW-65-85-D-0068. U.S. Army Corp of Engineers.
- Mitsch, William J., and Renee F. Wilson. 1996. "Improving the Success of Wetland Creation and Restoration with Know-How, Time, and Self-Design." *Ecological Applications* 6 (1): 77–83.
- Morgan-Jones, M., S. Bennett, and J.V. Kinsella. 1984. "The Hydrologic Effects of Gravel Winning in an Area West of London, United Kingdom." *Ground Water* Vol. 22 (No. 2): 154–61.
- National Research Council. 1992. *Restoration of Aquatic Ecosystems-Science, Technology, and Public Policy*. Washington D.C.: National Academy Press.
- Nelson, K.L. "Instream Sand and Gravel Mining." In *C.F. Bryan and D.A. Ritherford, Eds. Impacts on Warmwater Streams: Guidelines for Evaluation*, 189–96. Southern Division, America Fisheries Society. Little Rock, Arkansas.
- O'Rourke, D. 2001. "Conjunctive Use of the Brazos River Alluvium Aquifer". Final report: prepared for the Texas Water Development Board. HDR Engineering.
- Passarello, M. C., J. M. Sharp, and S. A. Pierce. 2012. "Estimating Urban-Induced Artificial Recharge: A Case Study for Austin, TX." *Environmental & Engineering Geoscience* 18 (1): 25–36.
- Pinkus, J. 1987. "Hydrogeologic Assessment of Three Solid Waste Disposal Sites on the Brazos River Alluvial Deposites". Unpub. master's thesis, Waco, TX.: Baylor University.
- Pollock, D.W. 1994. "User's Guide for MODPATH/MODPATH-PLOT, Version 3: A Particle Tracking Post-Processing Package for MODFLOW, the U.S. Geological Survey Finite-Difference Ground-Water Flow Model". U.S. Geological Survey Open-File Report 94-464, 6 ch.
- Rich, C.A. 1983. "The Necessary Involvement and Responsibility of Separate Entities in Planning and Performance of Aquifer Restoration." *Proceeding of the Third National Symposium on Aquifer Restoration and Ground-Water Monitoring*, 3–10.
- Shah, Sachin D, and Geological Survey (U.S.). 2007. "Hydrogeologic Characterization of the Brazos River Alluvium Aquifer, Bosque County to Fort Bend County, Texas". Reston, Va.: U.S. Geological Survey.

- Shah, Sachin D., Wade H. Kress, and Anatoly Legchenko. 2007. "Application of Surface Geophysical Methods, With Emphasis on Magnetic Resonance Soundings, to Characterize the Hydrostratigraphy of the Brazos River Alluvium Aquifer, College Station, Texas, July 2006—A Pilot Study". 2007-5203. U.S. Geological Survey.
- Shah, Sachin D., and Natalie A. Houston. 2007. "Geologic and Hydrogeologic Information for a Geodatabase for the Brazos River Alluvium Aquifer, Bosque County to Fort Bend County, Texas". 0196-1497. United States: U. S. Geological Survey : Reston, VA, United States.
- Stricklin, Fred L. 1961. "Degradational Stream Deposits of the Brazos River, Central Texas." *Geological Society of America Bulletin* 72 (1): 19.
- Urbanc, M., and M. Berg. 2005. "Gravel Plains in Urban Areas: Gravel Pits as an Element of Degraded Landscapes." *Acta Geographica Slovenica* 45 (2): 35–61.
- Winston, R.B. 2009. "ModelMuse-A Graphical User Interface for MODFLOW-2005 and PHAST: U.S. Geological Survey Techniques and Methods 6-A29."
- Wong, S.S. 2012. "Developing a Geospatial Model for Analysis of a Dynamic, Heterogeneous Aquifer: The Brazos River Alluvium Aquifer, Central Texas". Thesis (unpublished), Waco, Texas: Baylor University.
- Woodward-Clyde Construction. "Gravel Removal Studies in Arctic and Subarctic Alaska". Washington D.C.: U.S. Fish and Wildlife Service FES/OBS-80/80.
- Younger, Paul L., S.A. Banwart, and Robert S. Hedin. 2002. *Mine Water: Hydrology, Pollution, Remediation*. Springer.
- Zedler, Joy B., and John C. Callaway. 1999. "Tracking Wetland Restoration: Do Mitigation Sites Follow Desired Trajectories?" *Restoration Ecology* 7 (1): 69–73.
- Zohdy, A.A., G.P. Eaton, and D.R. Mabey. 1974. "Application of Surface Geophysics to Ground-Water Investigations." In *U.S. Geological Survey Techniques of Water-Resources Investigations Book 2*, 116.